İSTANBUL TECHNICAL UNIVERSITY ★ INSTITUTE OF INFORMATICS

FOREST FIRE ANALYSIS USING SATELLITE IMAGERY

M.Sc. Thesis by
Kerem ESEMEN

Department : Communication Systems

Programme : Satellite Communication and Remote Sensing

Thesis Supervisor: Prof. Dr. Filiz SUNAR

MAY 2011

FOREST FIRE ANALYSIS USING SATELLITE IMAGERY

M.Sc. Thesis by
Kerem ESEMEN
(705081009)

MAY 2011

İSTANBUL TEKNİK ÜNİVERSİTESİ ★ BİLİŞİM ENSTİTÜSÜ

UYDU GÖRÜNTÜLERİ İLE ORMAN YANGINI ANALİZİ

Yüksek Lisans Tezi
Kerem ESEMEN
(705081009)

Tezin Enstitüye Verildiği Tarih :   06 Mayıs 2011
Tezin Savunulduğu Tarih :   07 Haziran 2011

Tez Danışmanı :   Prof. Dr. Filiz SUNAR (İTÜ)
Diğer Jüri Üyeleri :   Prof. Dr. Derya MAKTAV (İTÜ)
Prof. Dr. Nüzhet Dalfes (İTÜ)

MAYIS 2011

PREFACE

Throughout this study carried out within İTÜ Institute of Informatics: Satellite Communication and Remote Sensing program, an application of remote sensing and GIS in a wildfire damage analysis and assessment scenario was performed

Concept of remote sensing has been a life changing enthusiasm for me since I have taken the first lecture from my advisor in 2003. Thus, I would like to express my deepest gratitude and thanks to Prof. Dr. Filiz Sunar for her guidance and help in all possible ways, enlightening my path in exploring my passion.

I would like to thank to my family for their endless patience and support, without which I could never be in where I stand.

May 2011   Kerem Esemen

                                                     Geomatics Engineer

TABLE OF CONTENTS

ABBREVIATIONS

AVHRR	: Advanced Very High Resolution Radiometer
CCD	: Charge Coupled Device
CCRS	: Canadian Centre for Remote Sensing
CNES	: Centre National d'Etude Spatiales
DEM	: Digital Elevation Model
DN	: Digital Number
DVI	: Difference Vegetation Index
ESA	: European Space Agency
ETM	: Enhanced Thematic Mapper
EVI	: Enhanced Vegetation Index
FBP	: Fire Behavior Prediction
FROS	: Forward Rate of Spread
GAC	: Global Area Coverage
GCP	: Ground Control Points
GIS	: Geographical Information System
GOES	: Geostationary Operational Environmental Satellite
GPS	: Global Positioning System
HH	: Horizontal Horizontal polarization
HRG	: High Resolution Geometric
HRV	: High Resolution Visible
HRPT	: High Resolution Picture Transmission
HRV	: High Resolution Visible
HRVIR	: High Resolution Visible IR
HV	: Horizontal Vertical polarization
IFOV	: Instantaneous Field of View
ISODATA	: Iterative Self-Organizing Data Analysis
IR	: Infrared
LAC	: Local Area Coverage
LWIR	: Long Wave Infrared
NIR	: Near Infrared
MODIS	: Moderate-Resolution Imaging Spectroradiometer
MS	: Multispectral Image
MSS	: Multispectral Scanner
MWR	: Microwave Radiometer
NASA	: National Aeronautics and Space Administration
NDVI	: Normalized Difference Vegetation Index
NOAA	: National Oceanic and Atmospheric Administration
PAN	: Panchromatic image
POES	: Polar Orbiting Environmental Satellites
PVI	: Perpendicular Vegetation Index
RMS	: Root Mean Square
RVI	: Simple Ratio Vegetation Index
SAR	: Synthetic aperture radar

SPOT   : Systeme Probatoire pour l'Observation de la Terre
SRTM   : Shuttle Radar Topography Mission
SWIR   : Short Wave Infrared
TIR   : Thermal Infrared
TM   : Thematic Mapper
TVI   : Transformed Vegetation Index
USGS   : U.S. Geological Survey
UV   : Ultraviolet
VNIR   : Visible and Near Infrared
VV   : Vertical Vertical polarization

TABLE LIST

FIGURE LIST

FOREST FIRE ANALYSIS USING SATELLITE IMAGERY

SUMMARY

Along the Mediterranean and southern Aegean regions of Turkey especially during July and August, high temperature combined with low humidity poses a grave danger for forest terrain in terms of wildfires. As the statistics verify that vast majority of the forest fires are human induced due to increasing demand for land, whether the cause of fire is natural or intentional the damage is rapid and should be monitored in stages of before, during and after. Remote sensing having a significant place in hazard monitoring and evaluation; is able to provide multispectral satellites images of the fire zones for analysis and information extraction.

Remote sensing and geographical information systems (GIS) together define a superior approach to fire monitoring and assessment. Especially for the stages of containment, damage analysis and monitoring, images acquired from remote sensing satellites provide synoptic data with rich spatial and spectral information. In case of a high risk fire zone an information system is able to integrate key features such as metrological, transportation, physical, ecological and logistic data to carry out containment plans beforehand as well as damage analysis after a possible fire.

Through out this study, an application of remote sensing and GIS in a wildfire damage analysis and assessment scenario was performed. Damage assessment for the wildfire that took place between July 31st and August 5th, 2008 effective at Antalya province, Manavgat and Serik municipalities was accomplished by processing a SPOT 4 satellite image and integrating with local forestry data within ArcGIS environment. Spectral analysis and NDVI transformation was applied on post fire SPOT 4 satellite image acquired on August 7th, 2008, having 20m spatial resolution. Multispectral classification methods were next applied and classification accuracy assessments were performed. After, geometric corrections were carried out for accurate area calculations; classification results are integrated with local forest management data within ArcGIS to perform further analysis.

Keywords: Remote Sensing, SPOT 4, NDVI, GIS, Antalya, Wildfire

UYDU GÖRÜNTÜLERİ İLE ORMAN YANGINI ANALİZİ

ÖZET

Ülkemizde Akdeniz ve güney Ege Bölgeleri'nde özellikle Temmuz ve Ağustos aylarında çok yüksek seviyelere ulaşan sıcaklıklar, düşük nem ile birleştiğinde orman alanları açısından tehlike arz etmektedir. Bununla birlikte istatistikler, günümüzde hızla artan arazi ihtiyacı doğrultusunda orman yangınlarının büyük bölümünün; her ne kadar önlem alınmaya çalışılsa da, insan kaynaklı olduğunu göstermektedir. İster doğal ister kasıtlı yolla meydana gelmiş olsun, kısa sürede çok büyük hasara yol açan orman yangınları; öncesi, esnası ve sonrası safhaları olmak üzere gelişen yeni uydu teknolojileri beraberinde analitik bir yöntem ile izlenmelidir. Afet yönetimi, uzaktan algılama uygulamaları içerisinde önemli bir yere sahip olup; günümüzde en sık meydana gelen doğal afetlerden biri olan orman yangınları, uydu görüntüleri ile etkili bir biçimde değerlendirilebilmektedir.

Uzaktan algılama ve coğrafi bilgi sistemleri (CBS) yangın izleme ve değerlendirme açısından birlikte üstün bir yaklaşım sağlar. Özellikle önleme, hasar analizi ve izleme aşamalarında uzaktan algılama uyduları ile elde edilen görüntüler zengin spektral ve mekansal bilgi içeren sinoptik bir veri seti sağlar. Yangın açısından yüksek risk faktörüne sahip orman alanları açısından değerlendirildiğinde, bir coğrafi bilgi sisteminin meteorolojik, fiziksel, ekolojik ve lojistik veriler gibi anahtar özelikleri bir arada işleme olanağı sağlaması, önleme ve erken müdahale planlarının oluşturulması yanı sıra, olası bir yangın sonuncunda oluşacak hasarın önceden analizi için imkan yaratır.

Bu çalışmada sürecinde, yangın sonrası hasar tespiti konulu uzaktan algılama ve CBS uygulaması gerçekleştirtmiştir. 31 Temmuz – 5 Ağustos 2008 tarihleri arasında Antalya ili, Manavgat ve Serik İlçelerinde etkili olan orman yangını, SPOT 4 uydu görüntüleri ve uzaktan algılama analiz teknikleri ile değerlendirilmiştir. 20 metre çözünürlüklü ham uydu veri setinin spektral analizi ardından, görüntüye NDVI dönüşümü uygulanmıştır. Ardından, tamamen gerçekleştirmiştir yanan ve kısmi hasar gören orman alanlarının miktarının tespitine yönelik sınıflandırma teknikleri uygulanarak, sınıflandırma doğrulukları hesaplanmıştır. Yanan ve hasarlı alanın doğru hesaplanması açısından önem taşıyan geometrik düzeltme işlemi ardından, sonuçlar mevcut dijital amenajman haritaları ile ArcGIS ortamında ilişkilendirilerek ileri analizler gerçekleştirilmiştir.

Anahtar sözcükler: Uzaktan Algılama, SPOT 4, NDVI, CBS, Antalya, Orman Yangını

1. INTRODUCTION

The nature consists of a delicate balance where actions of each and every being have an important affect one the other. As human population increases each year, the consequences of our involvement, either intentionally or unintentionally cause the degradation of this balance, resulting in severe natural hazards. While a global economy built on consumption without recycling demands more and more energy sources, the natural resources are being depleted and byproducts are accumulated not only as solid waste but also in form of aerosols in atmosphere, which evidently is the primary cause of the disturbance in climate known as global warming.

Forests, being referred as the lungs of the ecosystem, are the only natural stabilizer to sustain the fundamentals of life: Oxygen and carbon dioxide, in equilibrium. Occupying over 4 billion hectares of land, forest systems regulate the precipitation and underground waters, stand against erosion and soil degradation and provide a habitat for almost two thirds of all living species on Earth [1].
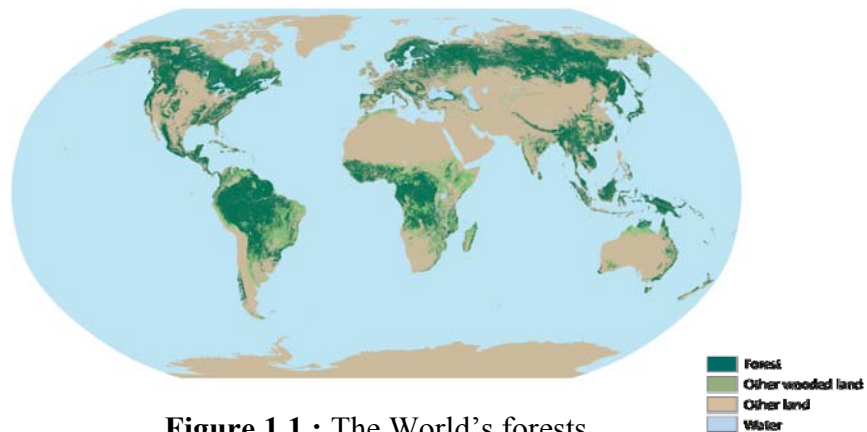
Figure 1.1 : The World's forests

Forest being such a vital ecosystem, are under a serious threat. Due to global warming, increased temperatures and decreased precipitation result in more dry fuel which amplifies the risk of natural fire occurrences. Moreover as human induced fires caused by carelessness or personal benefits, keeps threatening the forests; even a small fire can turn into a catastrophic wildfire in a fuel rich area due to increased duration and propagation as consequences of global warming.

In awareness of such threat, forest ecosystem has to be closely monitored against fires. Quick response should be given in case of a fire, accurately planning the containment and extinguishing procedures. Recurrent monitoring of previously damaged forest areas have to be performed; to effectively intervene in case of arson scenarios for personal gain in urbanization, and make rehabilitation as fast as possible. To accomplish these necessities in conventional methods, lot of time and manual labor are required thus it seems impossible to satisfactorily manage, however advancement in technology make it possible to detect, contain, analyze and monitor every stage of a forest fire faster, more accurate and recursively for either large or small areas.

Remote sensing and geographical information systems (GIS) are such technologies, defining a new better approach to fire monitoring and assessment. Especially for stages of containment, damage analysis and monitoring, images acquired from remote sensing satellites help to provide synoptic data with rich spatial and spectral information. In case of a high risk fire zone an information system can provide metrological, transportation, physical, ecological and logistic data to contain a probable fire as fast and harmless as possible. A skilled analyst can quickly extract the post fire damaged area information from a sufficient satellite image. Using the extracted information as layers in combination to the available data within a GIS, the analyst can provide a database for further inquiry of the damage cost effectively and quickly. Thus remote sensing data together with GIS are the key tools in analysis and monitoring of wildfires.

Through out this thesis, an application of remote sensing and GIS in a wildfire damage analysis and assessment scenario was performed. Damage assessment for the wildfire that took place between July 31st and August 5th, 2008 effective at Antalya province, Manavgat and Serik municipalities was accomplished by processing a SPOT 4 satellite image and integrating with local forestry data within ArcGIS environment. Spectral analysis and NDVI transformation was applied on post fire SPOT 4 satellite image acquired on August 7th, 2008, having 20m spatial resolution. Multispectral classification methods were next applied and classification accuracy assessments were performed. After geometric corrections were carried out for accurate area calculations, classification results are integrated with local forest management data within ArcGIS to perform further analysis.

2. FUNDAMENTALS OF REMOTE SENSING

Remote sensing is the science of acquiring information about the Earth's surface without actually being in contact with it. This is done by recording reflected or emitted energy by means of an air / space borne instrument equipped with an appropriate sensor. This data is later to be processed and analyzed to extract useful information [1]. Remote sensing technique consists of two components: "Data Acquisition" and "Data Processing". Data acquisition includes steps from initial electromagnetic illumination into image development on a ground station. Data processing steps are then applied correcting and transforming the image to be later interpreted and analyzed.

2.1 Components of the Remote Sensing

1. Energy Source or Illumination: An energy source which illuminates or provides electromagnetic energy to the target. For passive satellites, the sun is the source of energy; however active satellites such as radar or lidar carry the electromagnetic energy generators on themselves (Figure 2.1).

2. Radiation and atmospheric interference: The energy that travels from the source to the target interacting with the atmosphere and the environment in between.

3. Interactions with the ground target: The energy reaches the target and the interaction comes out that depends on the properties of both the target and the radiation.

4. Recording of the emitted / reflected energy by the sensor: Sensor collects and records the energy that has been scattered by, or emitted from the target.

5. Transmission, Reception and Processing: The energy recorded by the sensor is transmitted to processing station where the data are processed into an image.

6. Interpretation and analysis: The image is interpreted, visually, digitally or electronically.

7. Application: The image is processed to extract information about the target. Data can be integrated with data from other sources.
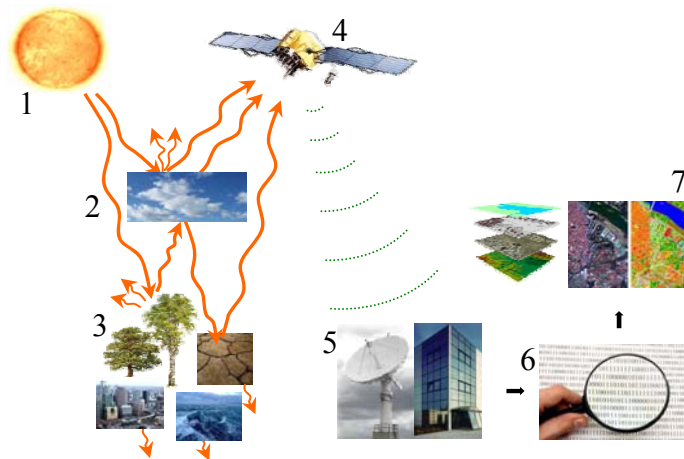
Figure 2.1 : Components of remote sensing

2.2 Electromagnetic Radiation and Spectrum

Electromagnetic radiation is the key to sensing the target in remote sensing systems. Either generated naturally by the Sun or artificially by an active sensor, its interactions with the atmosphere and the target surface determines the quality of the image from which interpretations are carried out. Energy moves at the speed of light, commonly referred to as c = 299,793 km/sec or c = 3 * 108 m/sec in vacuum, and can be described both as particles and as harmonic waves. An electromagnetic wave consists of two primary components that are an electric field and a magnetic field (Figure 2.2). The movement and properties of electromagnetic energy can be described in terms of velocity (c), wavelength (L), and frequency (f) [2].

$$L = \frac{c}{f} \qquad\qquad\qquad\qquad \textbf{(2.1)}$$
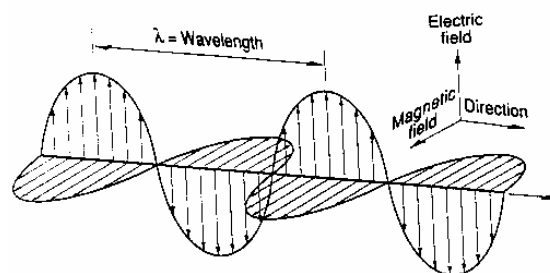
Figure 2.2 : The electromagnetic wave.

4

The electromagnetic spectrum is a continuum of all electromagnetic waves arranged according to frequency and wavelength. The sun, earth, and other bodies radiate electromagnetic energy of varying wavelengths. The micron is the basic unit for measuring the wavelength of electromagnetic waves. The spectrum of waves is divided into sections based on wavelength (Figure 2.3).
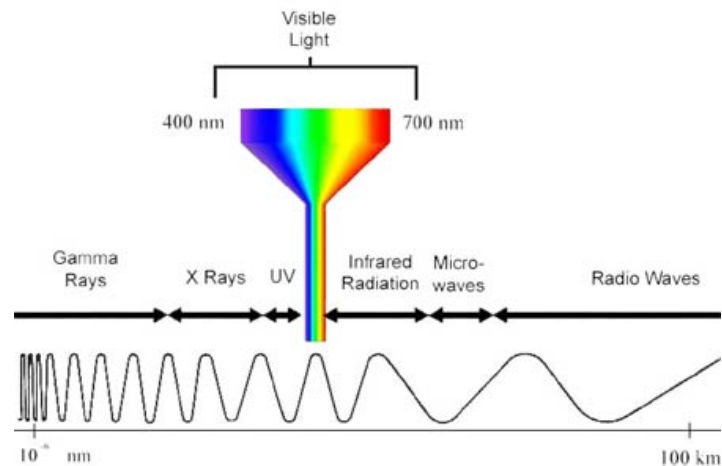
Figure 2.3 : The electromagnetic spectrum.

The shortest waves are gamma rays, which have wavelengths of 10e-6 microns or less, generated by radioactive atoms and in nuclear explosions [3]. X-ray is the highly penetrating rays of 10 nm wavelength that emanated when high energy electrons struck a metal target. The sun is a strong source of ultraviolet radiation, but atmospheric absorption eliminates most of the shorter wavelengths. The snow reflects UV while most other substances absorb it strongly. UV wavelength varies between 10nm and 400nm [4]. Visible light is the part of the electromagnetic spectrum which human eye can detect (Figure 2.4). Satellites with multispectral sensors are able to record in at least a portion of visible spectrum. The narrow visible part of the electromagnetic spectrum corresponds to the wavelengths near the maximum of the Sun's radiation curve. The range of visible consists of the narrow portion of the spectrum, from 400nm: Blue to 0.7nm: Red [5].
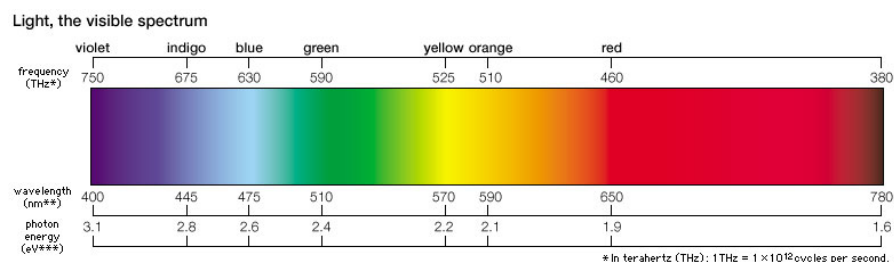
Figure 2.4 : The visible light spectrum

The term "infrared" refers to a broad range of frequencies, beginning at the microwave frequencies, extending up to the low frequency (red) end of the visible spectrum. The wavelength range is from about 1 mm down to 750 nm. The range adjacent to the visible spectrum is called near infrared and the longer wavelength part is called far infrared. Infrared in remote sensing, is referred as emitted energy, mostly from hot areas such as fires and volcanoes or living cells of plants and vegetation. Space borne sensors especially, are calibrated to respond to those intervals of infrared emission from vegetation in order to distinguish and classify them. The region of the spectrum that is composed of electromagnetic radiation with wavelengths between 1 mm and 300 cm is called microwave band. These levels are too low for high-resolution image generation. In order to this most microwave sensors can both generate and detect their own source of radiation. The longest of all with 10 cm to 10 km wavelengths, radio waves are one of the key components of remote sensing technology. Satellites are controlled by the commands carried on radio waves. The recorded data is also carried back to the ground station by radio waves [4].

2.3 Atmospheric and Target Surface Interactions

2.3.1 Atmospheric Interactions

As electromagnetic energy enters the Earth's atmosphere, it will be under the influence of absorption, refraction and scattering due to the presence of water molecules, particles and atmospheric gases with various density and transmittance. While some frequencies of electromagnetic waves are totally absorbed, some are to be scattered, reducing the energy and some will be transmitted with no loss. This sole depends on the length of the electromagnetic wave and the current atmospheric condition. The reliability of the system thus is limited with the atmospheric interactions, which generate the term "atmospheric windows" (Figure 2.5); unique band intervals where certain wavelengths are to be transmitted with no loss. Sensors calibrated accordingly will carry out the work with consistency.
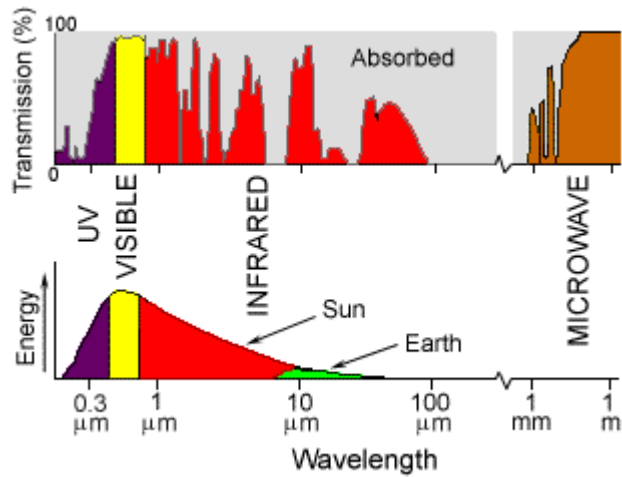
Figure 2.5 : The atmospheric window

Absorption is the one of the main mechanism at work when electromagnetic radiation interacts with the atmosphere. This phenomenon causes molecules in the atmosphere to absorb energy at various wavelengths. Ozone, carbon dioxide, and water vapor are the three main atmospheric constituents which absorb radiation. Ozone serves to absorb the ultraviolet radiation from the sun. Carbon dioxide referred to as a greenhouse gas, has a tendency to absorb radiation strongly in the far infrared portion of the spectrum which serves to trap this heat inside the atmosphere. Water vapor in the atmosphere absorbs much of the incoming long wave infrared and shortwave microwave radiation (between 22µm and 1m). The presence of water vapor in the lower atmosphere varies greatly from location to location and at different times of the year. The air mass above a desert would have very little water vapor to absorb energy, while the tropics would have high concentrations of water vapor due to high humidity [1].

Scattering occurs when particles or large gas molecules present in the atmosphere interact with and cause the electromagnetic radiation to be redirected from its original path. How much scattering takes place depends on several factors including the wavelength of the radiation, the quantity of particles or gases, and the distance the radiation travels through the atmosphere. There are three types of scattering which take place: Rayleigh, Mie and Non-selective scattering [1]. Rayleigh scattering occurs when particles are very small compared to the wavelength of the radiation such as small specks of dust or nitrogen and oxygen molecules, causing shorter wavelengths of energy to be scattered much more than longer wavelengths. Mie scattering occurs mostly in the lower portions of the atmosphere when the

particles are just about the same size as the wavelength of the radiation such as dust, pollen, smoke and water vapor which tends to affect longer wavelengths than those affected by Rayleigh scattering. Non-selective scattering occurs when the particles are much larger than the wavelength of the radiation such as water droplets and large dust particles resulting in all wavelengths to be scattered about [1].

2.3.2 Target Surface Interactions

51% electromagnetic radiation which is not absorbed or scattered during its travel through the Earth's atmosphere, is transmitted down, reaching the target surface. 47% of this energy is absorbed by the Earth's Surface later to be emitted as infrared radiation, leaving a 4% to reflect back into the atmosphere and the sensor. As energy can not be destroyed nor created, it has to be conserved. Thus the incident energy $E_I(\lambda)$ has to be equal to sum of reflected $E_R(\lambda)$, absorbed $E_A(\lambda)$, and transmitted $E_T(\lambda)$ energy (Figure 2.6).
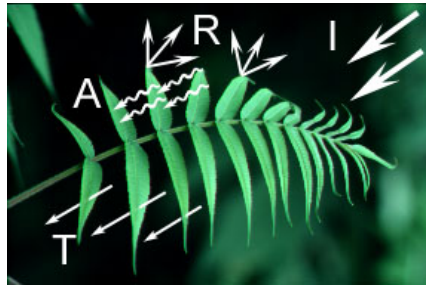
Figure 2.6 : Target surface interactions
Absorbance (A), Transmittance (T), Reflectance (R) and Incident Energy (I)

$$E_I(\lambda) = E_R(\lambda) + E_A(\lambda) + E_T(\lambda) \tag{2.2}$$

$$1 = \frac{E_R(\lambda)}{E_I} + \frac{E_A(\lambda)}{E_I} + \frac{E_T(\lambda)}{E_I} \tag{2.3}$$

$$1 = r(\lambda) + a(\lambda) + t(\lambda) \tag{2.4}$$

This is has an important role in distinguishing between surface materials. Even within the same feature type, and because of the wavelength dependency, the proportion of reflected, absorbed, and/or transmitted energy varies at different wavelengths, causing two features which are indistinguishable in one spectral range to be different in another wavelength band. These spectral variations result in the effect of color [6]. Reflectance also depends on the geometrical shape of the surface.

Reflecting behavior of an object is characterized by the surface roughness in comparison to the wavelength of incident energy.

Specular Reflectance is of little use in remote sensing because the incoming energy is completely reflected in another direction (Figure 2.7). Surface particles are small relative to the wavelength. Light is reflected in a single direction and it is also called mirror reflection. Still water, ice and many other minerals with crystal surfaces have the same property and they mostly seen black.

Diffuse reflections contain spectral information on the color of the reflecting surface. Remote sensing is mostly interested in measuring the diffuse reflectance properties of terrain features. Surface is rough relative to the incident wavelength. It is also called isotropic reflection because the energy is reflected equally in all directions (Figure 2.7). Many natural surfaces act as a diffuse reflector to some extent. A perfectly diffuse reflector is termed as Lambertian surface because reflective brightness is same when observed from any angle.
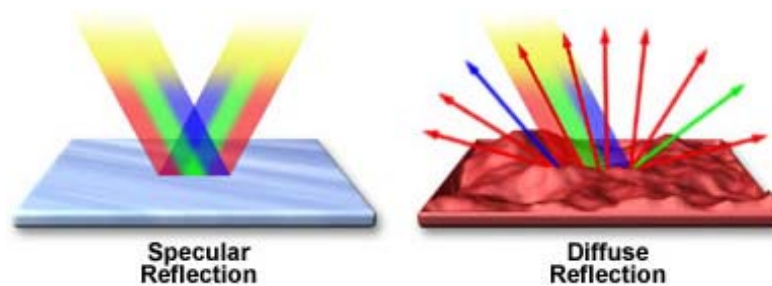
Figure 2.7 : Specular Reflectance and Diffuse Reflectance

The reflectivity of a surface can also be measured for a specific wavelength or for the entire electromagnetic spectrum. The spectral reflectance of an object is the percentage of electromagnetic radiance reflected by the object in a specific wavelength or spectral band. The reflectance of an object aggregated over a broader segment of the electromagnetic spectrum or over the entire spectrum is called the albedo of an object. The higher the albedo, the more reflective the surface and the brighter the surface will appear in remotely sensed imagery. The range can vary from 0 to 100%. Different objects may have similar albedo, measured over a broad portion of the electromagnetic spectrum but may still have very different patterns of reflectance within narrow spectral bands. These differences can be used to discriminate between different types of objects [7].

9

2.4 Spectral Signatures

Spectral reflectance is the portion of incident radiation that is reflected by a non-transparent surface. The fraction of energy reflected at a particular wavelength varies for different features. Additionally, the reflectance of features varies at different wavelengths. A spectral signature is a unique reflectance value in a specific part of the spectrum. In order to this two features that are indistinguishable in one spectral range may be very different in another portion of the spectrum. This is an essential property of matter that allows for different features to be identified and separated by their spectral reflectance signatures (Figure 2.8).
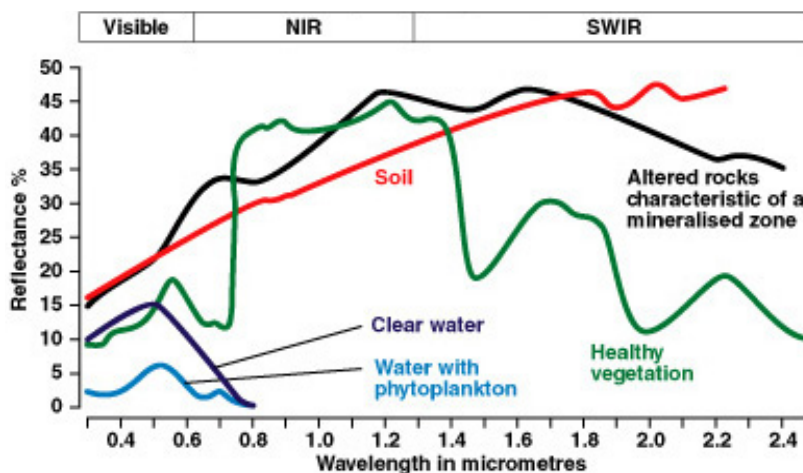
Figure 2.8 : Spectral reflectance curve examples

Spectral signatures for different surfaces can be obtained using a device called a spectrometer. The spectrometer detects the electromagnetic radiation reflected off a surface in a specified spectral band. By measuring reflectance in many different bands, the spectral signature over the full range of wavelengths can be obtained [7]. For any given material, the amount of solar radiation that is reflected (absorbed, transmitted) will vary with wavelength. This important property of matter allows us to separate distinct cover types based on their response values for a given wavelength. The spectral signature of a certain land cover is defined by plotting its response characteristics against wavelength [8]. Although each and every single matter has a unique spectral reflectance, the most frequent ones to be observed are grouped under 3 similar reflectance characteristics of soil, water and green vegetation.

2.4.1 Spectral Reflectance of Vegetation

There are several factors that influence the reflectance quality of vegetation on remote sensing images. These include brightness, greenness and moisture. Brightness is calculated as a weighted sum of all the bands and is defined in the direction of principal variation in soil reflectance. Greenness is orthogonal to brightness and is a contrast between the near-infrared and visible bands. It is related to the amount of green vegetation in the scene. Moisture in vegetation will reflect more energy than dry vegetation [8].

Vegetation has a unique spectral signature which enables it to be distinguished readily from other types of land cover in an optical/near-infrared image [9].What may differ for each specie, is the typical spectral features recorded for the three main optical spectral domains; leaf pigments, cell structure and water content (Figure 2.9).

Electromagnetic wavelengths affect different parts of plant and trees. These parts include leaves, stems, stalks and limbs of the plants and trees. The length of the wavelengths also plays a role in the amount of reflection that occurs. Tree leaves and crop canopies reflect more in the shorter radar wavelengths, while tree trunks and limbs reflect more in the longer wavelengths. The density of the tree or plant canopy will affect the scattering of the wavelengths [10].

Leaf properties that influence the reflectance values are the internal / external structure, age, water content, mineral stresses, and healthiness. The spectral reflectance curve shows relatively low values in the red and blue portions of the visible spectrum, with a peak in the green spectral band. There is a slight reflectance peak in green and which is the reason that growing vegetation appears green due to the chemical compound in leaves; the chlorophyll strongly absorbs radiation in the red and blue wavelengths. Generally %70-%90 of blue and red light is absorbed to provide energy for the process of photosynthesis. Leaves appear greenest, when chlorophyll content is at its maximum. In autumn, there is less chlorophyll in the leaves, so there is less absorption and proportionately more reflection of the red wavelengths.
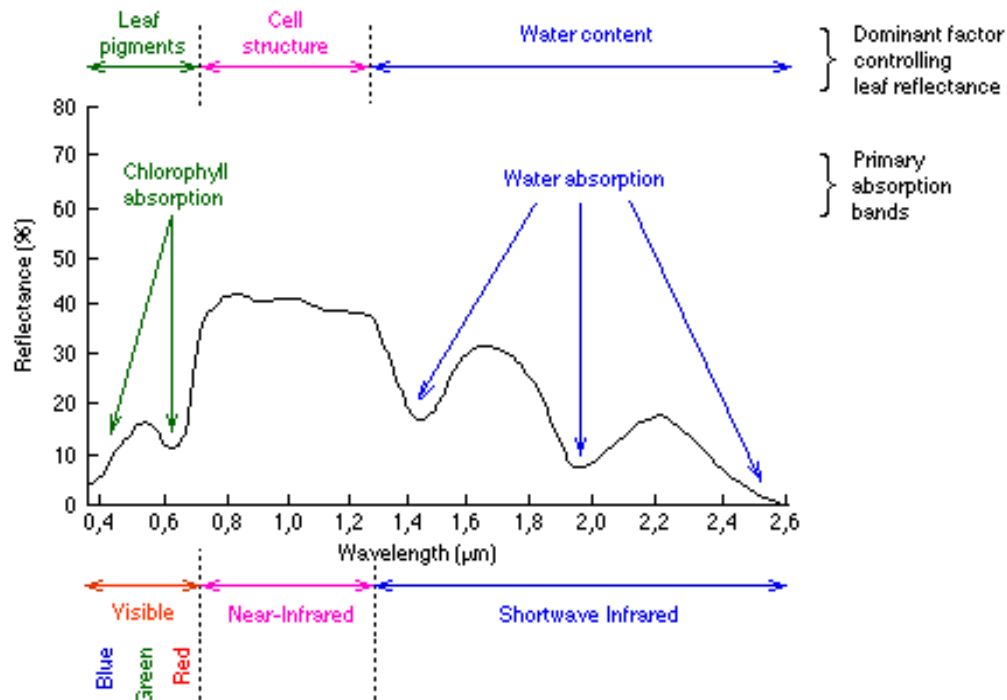
Figure 2.9 : Spectral reflectance properties of green vegetation

Electromagnetic wavelengths affect different parts of plant and trees. These parts include leaves, stems, stalks and limbs of the plants and trees. The length of the wavelengths also plays a role in the amount of reflection that occurs. Tree leaves and crop canopies reflect more in the shorter radar wavelengths, while tree trunks and limbs reflect more in the longer wavelengths. The density of the tree or plant canopy will affect the scattering of the wavelengths [10].

The internal structure of healthy leaves act as excellent source of emission in near-infrared wavelengths. Cell structures are dominant in near infrared portion and this region is suitable to discriminate the vegetation type. Measuring and monitoring the near-infrared value is a way to determine how healthy vegetation may be.

As the plant grows older the reflection value in the near infrared portion decreases whereas the reflectance of visible portion remains not affected. If there is something wrong with the cell structure this will affect the reflectance and the reflectance will become lesser in unhealthy vegetation type. When the leaf gets thicker the water component will increase relatively and this will also cause less reflection.

The reflectance of vegetation in the SWIR region is more varied, depending on the types of plants and the plant's water content. Water has strong absorption bands around 1.45, 1.95 and 2.50 µm. Outside these absorption bands in the SWIR region,

reflectance of leaves generally increases when leaf liquid water content decreases (Figure 2.9). This property can be used for identifying tree types and plant conditions from remote sensing images. The SWIR band can be used in detecting plant drought stress and delineating burnt areas and fire-affected vegetation. The SWIR band is also sensitive to the thermal radiation emitted by intense fires, and hence can be used to detect active fires, especially during night-time when the background interference from SWIR in reflected sunlight is absent [9].

2.4.2 Spectral Reflectance of Water

The reflectance properties of water are a function of the water and the organic and/or inorganic material in the water. If there is a large amount of suspended sediment present, then a higher visible reflectance will result when compared to clear water bodies. The amount of chlorophyll will also affect the amount of water reflectance. An increase in chlorophyll will result in a decrease of blue wavelengths and increase in green wavelengths, which enables monitoring the presence and estimate the concentration of algae. Temperature variations affect the reflectance of water throughout the day. Presence of turbulence, currents and surface waves will cause a diffuse reflection, also affecting the amount of energy absorbed and transmitted.

The most distinctive characteristic of water, with reference to spectral reflectance, is the energy absorption at the near-infrared wavelengths. The incident energy interacts in a complex manner such as, interactions with the water's surface is in a form of specular reflectance but, in combination with the refracted and then reflected energy from the material suspended in a bottom of a water body. Certain water characteristics such as dissolved oxygen concentration, pH, salt concentration, can not be observed directly with water reflectance changes but can be correlated with observed reflectance. Thus reflectance data for water bodies has been used to detect pollutants like oil or industrial wastes, and used to determine the presence or absence of tannin dyes from the swamp vegetation in lowland areas [10].

2.4.3 Spectral Reflectance of Soil

There are several different areas involved in remote sensing of soils. Satellite imagery will provide the visible boundaries of soil types, while remote sensing will provide for a shallow penetration of soils. Spectral signatures for the soil surfaces provide additional physical data. Interpreting the remote sensing images and the

spectral signatures allow for the classification of the soil types. Four main factors influence the soil reflectance in remote sensing images: mineral composition, soil moisture, organic matter content and soil texture (surface). Size and shape of the soil aggregate also influence the reflectance in the images.

The mineral composition of soil affects the reflectance spectrum. Increasing reflectance of soils occurs from the visible to the shortwave infrared - with absorption bands around 1.4 um and 1.9 um related to the amount of moisture in the soil (Figure 2.10). Radar waves may not be able to penetrate soil if it is moist. On the soil reflectance spectra, this soil moisture will develop parallel curves. Moisture of soil has an equal effect over the spectrum and the ration between the spectral bands. Spectral bands of red and near-infrared bands are independent from the soil moisture.
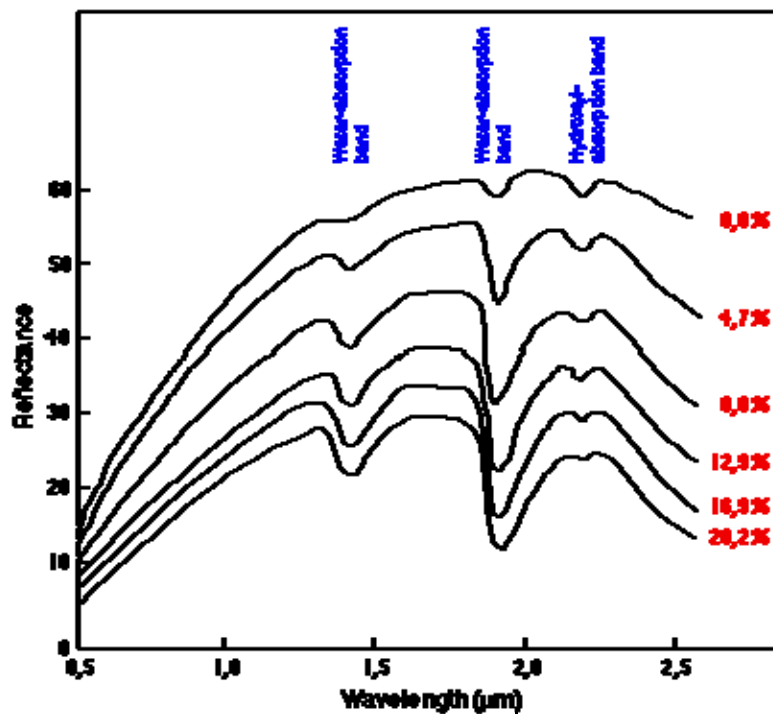
Figure 2.10 : Spectral reflectance curves for soil for various humidity percentages

Organic matter is the third factor that influences soil optical properties. Organic matter may indirectly affect the spectral influence, based on the soil structure and water retention capacity. High organic matter in soil may produce spectral interferences for band characteristics of minerals like Mn and Fe. Soil texture (roughness) also affects soil optical properties. Light is trapped in the rough surfaces of the coarse soil particles. If iron and lime are present, a stronger reflectance is

received than if the soil material was fine textured and dry. Variations in soil reflectance occur where there is a change in distribution of light and shadow areas with surface roughness areas. This factor is important in the thermal infrared and microwave spectral domains. Soil size and shape influence the reflectance properties. If the size of a soil aggregate expands in diameter, a decrease in reflection will result. Soil temperatures and changes in structure are also recorded. The shape is related to the surface (texture); a smooth, even surface will probably result from a more smooth soil compound, instead of a rough one [10].

3. REMOTE SENSING SATELLITE SYSTEMS

A satellite, by definition is a body orbiting around another body. In terms of remote sensing, a satellite system is a space born carrier mounted with radiometric sensors, orbiting around the Earth at a constant altitude, providing imagery for research and operational applications. Space borne remote sensing provides large area coverage, frequent and repetitive coverage of an area of interest, quantitative measurement of ground features using radiometrically calibrated sensors, semi-automated computerized processing and analysis and relatively lower cost per unit area of coverage as an advantage with respect to airborne imaging systems [9].

3.1 Satellite Orbits

A satellite follows a generally elliptical orbit around the earth. The time taken to complete one revolution of the orbit is called the orbital period. The satellite traces out a path on the earth surface, called its ground track, as it moves across the sky. As the earth below is rotating, the satellite traces out a different path on the ground in each subsequent cycle. Remote sensing satellites are often launched into special orbits such that the satellite repeats its path after a fixed time interval. This time interval is called the repeat cycle of the satellite [9]. There are there types of orbits for a satellite to track that are geostationary, near Polar and sun synchronous orbits.

If a satellite follows an orbit parallel to the equator in the same direction as the earth's rotation and with the same period of 24 hours, the satellite will appear stationary with respect to the earth surface. This is a geostationary orbit (Figure 3.1a). Satellites in the geostationary orbits are located at a high altitude of 36,000 km. These orbits enable a satellite to always view the same area on the earth. A large area of the earth can also be covered by the satellite. The geostationary orbits are commonly used by meteorological satellites [9].

When the orbital plane is inclined at a small angle with respect to the earth's rotation axis it is called a near polar orbit (Figure 3.1b). A satellite following a properly

designed near polar orbit passes close to the poles and is able to cover nearly the whole earth surface in a repeat cycle [9].

| (a) | (b) |
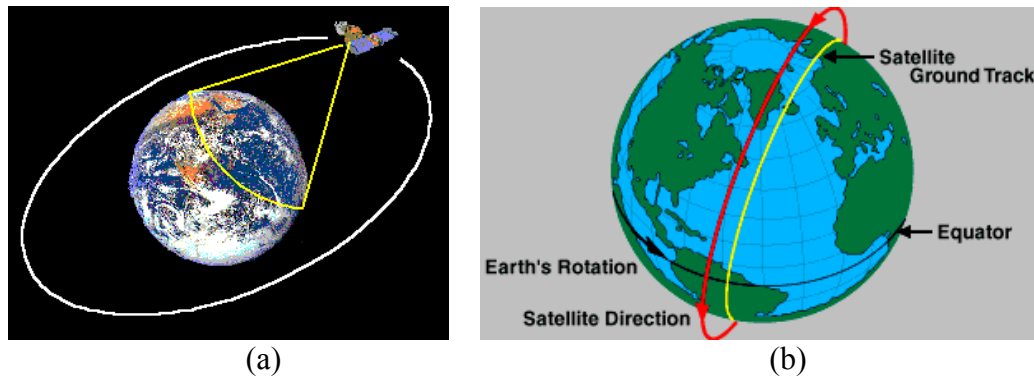
Figure 3.1 : a) Geostationary Orbit b) Near Polar – Sun Synchronous Orbit

Earth observation satellites however, usually follow the sun synchronous orbit. A sun synchronous orbit is a near polar orbit whose altitude is such that the satellite will always pass over a location at given latitude at the same local solar time (Figure 3.1b). In this way, the same solar illumination condition; except for seasonal variations can be achieved for the images of a given location taken by the satellite [9].

3.2 Earth Observation Satellite Systems

A number of remote sensing satellites are currently available, providing imagery suitable for various applications. Each of these satellite-sensor platforms are characterized by the wavelength bands employed in image acquisition, spatial resolution of the sensor, the coverage area and the temporal converge [9].

In terms of the spatial resolution, the satellite imaging systems can be classified into:

- Low resolution systems (approx. 1 km or more)

- Medium resolution systems (approx. 100 m to 1 km)

- High resolution systems (approx. 5 m to 100 m)

- Very high resolution systems (approx. 5 m or less)

In terms of the spectral regions used in data acquisition, the satellite imaging systems can be classified into:

- Optical imaging systems including visible, near infrared and shortwave infrared systems

- Thermal imaging systems

- Synthetic aperture radar (SAR) imaging systems

Optical / thermal imaging systems can be classified according to the number of spectral bands used:

- Monospectral or panchromatic systems: Single wavelength band and grayscale image

- Multispectral systems: Includes several spectral bands

- Superspectral systems: Includes tens of spectral bands

- Hyperspectral systems: Includes hundreds of spectral bands

Synthetic aperture radar imaging systems can be classified according to the combination of frequency bands and polarization modes used in data acquisition:

- Single frequency: L-band, C-band, X-band

- Multiple frequency : combination of two or more frequency bands

- Single polarization: (VV, HH, HV).

- Multiple polarizations: Combination of two or more polarization modes.

3.2.1 LANDSAT Earth Observation Satellites

The LANDSAT program consists of a series of optical/infrared remote sensing satellites for land observation. The program was first started by The National Aeronautics and Space Administration (NASA) in 1972, then turned over to the National Oceanic and Atmospheric Administration (NOAA) after it became operational. The first satellite in the series, LANDSAT-1, initially named as the Earth Resource Technology Satellite ERTS-1 was launched on 23 July 1972. The satellite had a designed life expectancy of 1 year but it ceased operation on January 1978. LANDSAT-2 was launched on 22 January 1975 and three additional LANDSAT satellites were launched in 1978, 1982, and 1984 as LANDSAT-3, 4, and 5 respectively. LANDSAT-6 was launched on October 1993 but the satellite failed to

obtain orbit (Table 3.1). LANDSAT-7 was launched in 15 April 1999. Currently, only LANDSAT-5 and 7 are operational [9].

Table 3.1: LANDSAT orbit specifications

Type	Sun-Synchronous
Altitude	705 km
Inclination	98.2°
Period	99 min
Repeat Cycle	16 days (233 orbits)

Multi-Spectral Scanner (MSS) is deployed on LANDSAT-1 to 5. Being one of the older generation sensors, routine data acquisition for MSS was terminated in late 1992. The resolution of the MSS sensor was approximately 80 m with radiometric coverage in four spectral bands. Spectral and spatial characteristics of MSS sensor are given in Table 3.2 and Table 3.3 respectively.

Table 3.2: LANDSAT MSS spectral characteristics

Band Landsat 1,2, 3	Band Landsat 4, 5	Spectral Range (Microns)	EM Region	Generalized Application Details
4	1	0.5 - 0.6	Visible Green	Assessment of vegetation vigor, coastal mapping
5	2	0.6 - 0.7	Visible Red	Chlorophyll absorption for vegetation differentiation
6	3	0.7 - 0.8	Near Infrared	Delineation of water bodies, biomass surveys
7	4	0.8 - 1.1	Near Infrared	Delineation of water bodies, biomass surveys

Table 3.3: LANDSAT MSS spatial characteristics

Swath width		184 × 185.2 km
Ground Sampling Interval (pixel size)	Landsat 1-3	57 × 79 m
Quantization		6 bit (64 levels)
Ground Sampling Interval (pixel size)	Landsat 4, 5	57 × 82 m
Quantization		8 bit (256 levels)

Thematic Mapper (TM) has first been operational on LANDSAT-4. TM sensors primarily detect reflected radiation from the Earth surface in the visible and near-infrared (IR) wavelengths, but the TM sensor provides more radiometric information than the MSS sensor. Enhanced Thematic Mapper Plus (ETM+) is carried on board with Landsat 7. The ETM+ instrument is an eight-band multispectral scanning radiometer capable of providing high-resolution image information of the Earths surface. Its spectral bands are similar to those of TM, except that the 6th band with thermal wavelength has an improved resolution of 60 m with respect to 120 m in TM. There is also an additional panchromatic band at 15 m resolution [11]. Spectral and spatial characteristics for TM and ETM+ sensors are given in Table 3.4 and Table 3.5 respectively.

Table 3.4: LANDSAT TM, ETM+ spectral characteristics

Band	Spectral Range	EM Region	Generalized Application Details
1	0.45 - 0.52	Visible Blue	Coastal mapping, soil - vegetation separation
2	0.52 - 0.60	Visible Green	Assessment of vegetation vigor
3	0.63 - 0.69	Visible Red	Chlorophyll absorption band
4	0.76 - 0.90	Near Infrared	Biomass surveys and delineation of water
5	1.55 – 1.75	Middle Infrared	Vegetation and soil moisture measurements; differentiation between snow and cloud
6	10.40- 12.50	Thermal Infrared	Thermal mapping, soil moisture studies and plant heat stress measurement
7	2.08 - 2.35	Middle Infrared	Hydrothermal mapping
8 (ETM+)	0.52 - 0.90 (pan)	Green – Near-IR	Large area mapping, urban change studies

Table 3.5: LANDSAT TM, ETM+ spatial characteristics

Property		Landsat 5 TM	Landsat 7 ETM+
Swath width		185 km	185 km
Ground Sampling Interval (pixel size)	Bands 1-5 & 7 Band 6 Band 8	30 × 30 m 120 × 120 m N/A	30 × 30 m 60 × 60 m 15 × 15 m (18 × 18 m GSI)
Quantization		8 bit (256 levels)	8 bit (256 levels)

3.2.2 The SPOT Satellite System

The SPOT program consists of a series of optical remote sensing satellites with the primary mission of obtaining Earth imagery for land use, agriculture, forestry, geology, cartography, regional planning, water resources and GIS applications (Figure 3.2.). The SPOT satellites are operated by the French Space Agency [9].
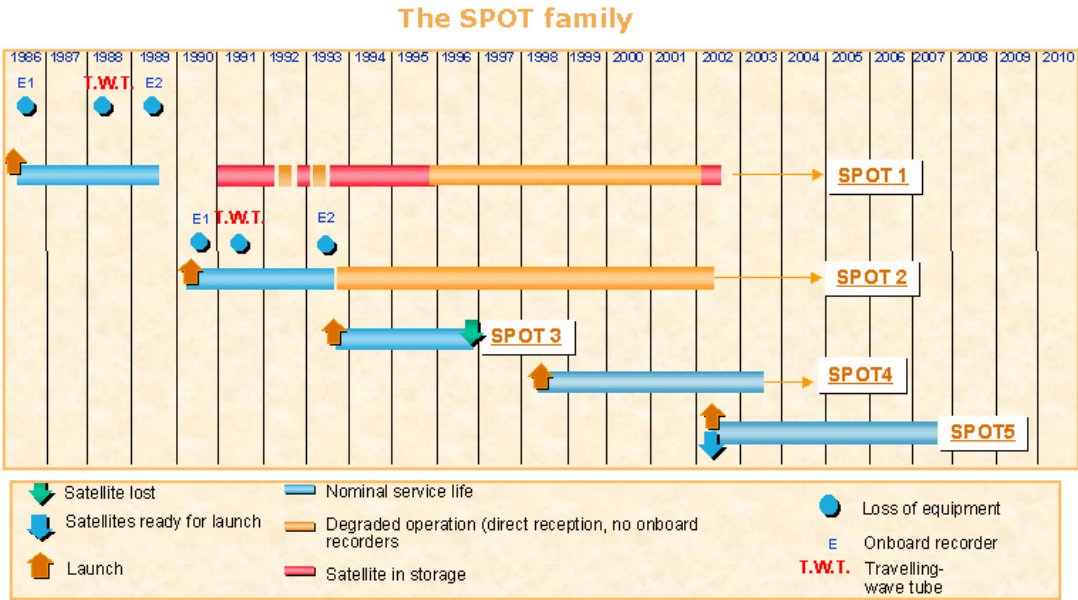
Figure 3.2 : SPOT Satellite System timeline and design lifetime

SPOT 1 satellite is launched into orbit on 22 February 1986 (Table 3.6). The SPOT 2 satellite is launched on 22 January 1990. Identical to its predecessor, SPOT 2 is the first in the series to carry the DORIS precision positioning instrument. SPOT 3 followed on 26 September 1993. It also carried the DORIS instrument, plus the American passenger payload POAM II, used to measure atmospheric ozone at the poles. SPOT 1 and SPOT 2 are still operational. SPOT 3 failed in 1996, having reached the end of its nominal mission lifetime.

SPOT 4 launched on 24 March 1998, features significant improvements over its predecessors, including a longer five-year design lifetime and enhanced imaging telescope features and recording capabilities. A spectral band in the short-wave-infrared is added and the panchromatic band configured as 0.61-0.68 μm, which acquires images on request at 10-metre or 20-metre resolution.

SPOT 5, the fifth satellite in the series, is orbited on the 4 May 2002 offering improved ground resolutions of 10 m in multispectral mode and 2.5 to 5 m in panchromatic and infrared mode. Higher 2.5 m resolution is achieved using a

sampling concept called Supermode. Featuring a new High Resolution Stereoscopic (HRS) imaging instrument operating in panchromatic mode, stereo pair images can be acquired to produce digital elevation models and generate orthorectified images [12].

Table 3.6: SPOT orbit specifications

Type	Near-Polar
Altitude at equator	822 km
Inclination	98.7°
Orbital period	101.4 min
Orbital cycle	26 days
Revisit interval	2 to 3 days

Two data acquisition modes for imaging purposes are employed as panchromatic (P) and multispectral (XS). HRV on the SPOT 1, 2 satellites (Table 3.7) and HRVIR on the SPOT 4 satellite (Table 3.8) can both operate in either mode, either simultaneously or individually.

Panchromatic (P) mode, imaging is performed in a single spectral band, corresponding to the visible part of the electromagnetic spectrum. The panchromatic band in SPOT 1, 2 HRV covers 0.51 to 0.73 μm. For SPOT 4 HRVIR, the panchromatic band is has a narrower bandwidth centered at the red band (0.61 to 0.68 μm). The panchromatic mode of the SPOT 4 HRVIR is named as the Monospectral (M) mode, to differentiate it from the panchromatic mode of the SPOT 1, 2 HRV. The single channel imaging mode (P or M mode) supplies only black and white images with a pixel width of 10 m. This band is intended primarily for applications calling for fine geometrical detail.

Multispectral imaging is performed by three spectral bands in green, red and near infrared spectrum in SPOT 1 and 2 HRV. There is a fourth band in SPOT 4 HRVIR in short-wave infrared spectrum. By combining the data recorded in these channels, color composite images can be produced with a pixel size of 20 meters.

Table 3.7: HRV spectral and spatial characteristic

Mode	Band	Wavelength (µm)	Resolution (m)
Multispectral	XS1	0.50 - 0.59 (Green)	20
Multispectral	XS2	0.61 - 0.68 (Red)	20
multispectral	XS3	0.79 - 0.89 (Near IR)	20
Panchromatic	P	0.51 - 0.73 (Visible)	10

Table 3.8: HRVIR spectral and spatial characteristic

Mode	Band	Wavelength (µm)	Resolution (m)
Multispectral	XI1	0.50 - 0.59 (Green)	20
Multispectral	XI2	0.61 - 0.68 (Red)	20
Multispectral	XI3	0.79 - 0.89 (Near IR)	20
Multispectral	XI4	1.53 - 1.75 (SWIR)	20
Monospectral	M	0.61 - 0.68 (Red)	10

The SPOT 4 & 5 satellites carry an on-board a low-resolution wide-coverage Vegetation instrument for monitoring the continental biosphere and to monitor crops. The Vegetation instrument provides global coverage on an almost daily basis at a resolution of 1 kilometer, enabling the observation of long-term changes on a regional and worldwide scale [9]. Spectral and spatial characteristics for Vegetation instrument are given in Table 3.9 and Table 3.10 respectively.

Table 3.9: Vegetation instrument spectral characteristic

Band	Wavelength (µm)
Blue	0.43 - 0.47
Red	0.61 - 0.68
Near-infrared	0.78 - 0.89
Short-wave infrared	1.58 - 1.75

Table 3.10: Vegetation instrument spatial characteristic

Swath width	2250 km
Ground Sampling Interval (pixel size)	1 km
Quantization	8 bit (256 levels)

3.2.3 NOAA Satellite System: AVHRR Instrument

NOAA is a series of polar orbiting environmental satellites (POES) operated by the United States National Oceanographic and Atmospheric Administration (NOAA). Advanced Very High Resolution Radiometer (AVHRR) is one of the main instruments carried on the NOAA satellites designed primarily for observation of clouds, land and sea surface at 1 km resolution in visible and infrared wavelengths .

The first AVHRR instrument was a 4-channel radiometer, carried on TIROS-N. This was subsequently improved to a 5-channel (visible to thermal infrared) instrument: AVHRR/2, carried on NOAA-7, 9, 10, 11 and 12 satellites. Starting from NOAA-14, the latest installment AVHRR/3 has an extra band in the shortwave infrared spectrum. This band shares the same transmission channel with the mid-wave infrared band designated as Band 3B and shortwave infrared band, Band 3A (Table 3.11). Only one of the 3A or 3B bands is activated at any instant [13].

Table 3.11 AVHRR spectral characteristics

Band	Wavelength (μm)	Applications
1 (Visible)	0.58 - 0.68	Cloud, snow and ice monitoring
2 (Near IR)	0.725 - 1.10	Water, vegetation and agriculture surveys
3A (Short Wave IR)	1.58 - 1.64	Snow, ice and cloud discrimination
3B (Medium Wave IR)	3.55 - 3.93	Sea surface temperature, volcano, forest fire activity
4 (Thermal IR)	10.3 - 11.3	Sea surface temperature, soil moisture
5 (Thermal IR)	11.3 - 12.5	Sea surface temperature, soil moisture

AVHRR data are acquired in three formats: High Resolution Picture Transmission (HRPT), Local Area Coverage (LAC) and Global Area Coverage (GAC). HRPT data are full resolution image data transmitted to a local ground station as they are being collected. LAC are also full resolution data, but recorded with an on-board tape recorder for subsequent transmission during a station overpass. GAC data provide daily subsampled global coverage recorded on the tape recorders and then transmitted to a ground station [13].

3.2.4 Terra and Aqua Satellite Systems: MODIS Instrument

The Moderate Resolution Imaging Spectroradiometer (MODIS) is an instrument measuring visible and infrared radiation to derive products ranging from vegetation, land surface cover, and ocean chlorophyll fluorescence to cloud and aerosol properties, fire occurrence, snow cover on the land, and sea ice cover on the oceans. The first MODIS instrument was launched on board the Terra satellite in December 1999, and the second was launched on Aqua in May 2002 [14]. The MODIS instrument provides 12 bit radiometric sensitivity in 36 spectral bands ranging from 0.4 μm to 14.4 μm wavelengths (Table 3.12). A ±55° scanning pattern at the altitude of 705 km achieves a 2,330 km swath [15]. Terra's orbit around the Earth is timed so that it passes from north to south across the equator in the morning, while Aqua passes south to north over the equator in the afternoon hence Terra MODIS and Aqua MODIS together enables viewing the entire Earth's surface every 1 to 2 days [16].

Table 3.11: MODIS spectral characteristics

Band	Wavelength (nm)	Resolution (m)	Primary Use	Band	Wavelength (μm)	Resolution (m)	Primary Use
1	620 - 670	250	Land / Cloud / Aerosols Boundaries	20	3.660 - 3.840	1000	Surface / Cloud Temperature
2	841 - 876			21	3.929 - 3.989		
3	459 - 479	500	Land / Cloud / Aerosols Properties	22	3.929 - 3.989		
4	545 - 565			23	4.020 - 4.080		
5	1230 - 1250			24	4.433 - 4.498		Atmospheric Temperature
6	1628 - 1652			25	4.482 - 4.549		
7	2105 - 2155			26	1.360 - 1.390		Cirrus Clouds Water Vapor
8	405 - 420	1000	Ocean Color / Phytoplankton / Biogeochemistry	27	6.535 - 6.895		
9	438 - 448			28	7.175 - 7.475		
10	483 - 493			29	8.400 - 8.700		Cloud Properties
11	526 - 536			30	9.580 - 9.880		Ozone
12	546 - 556			31	10.780 - 11.280		Surface / Cloud Temperature
13	662 - 672			32	11.770 - 12.270		
14	673 - 683			33	13.185 - 13.485		Cloud Top Altitude
15	743 - 753			34	13.485 - 13.785		
16	862 - 877			35	13.785 - 14.085		
17	890 - 920		Atmospheric Water Vapor	36	14.085 - 14.385		
18	931 - 941						
19	915 - 965						

4. DIGITAL IMAGE PROCESSING TECHNIQUES

An image is a two dimensional representation of objects from a three dimensional scene. Digital, refers to numerical values. Thus digital image stands for numerical representation of an object on a two dimensional surface by breaking it up into individual picture elements called pixels and assigning each element a value within a specific range to represent the corresponding intensity in the three dimensional world. A digital image consists of rows and columns of pixel, each with an integer value called Digital Number, representing the brightness value of associated region of the object (Figure 4.1). As in remote sensing procedures, images are recorded in digital forms and processed by the computers to produce images for interpretation purposes [2].

The sensor deployed on remote sensing satellite, detects the reflected or emitted energy from its target, translating the acquired intensity into an array of numbers that a computer can recognize. However, each system provides images with different qualities. The influential factor that determines the image quality is called the Resolution.
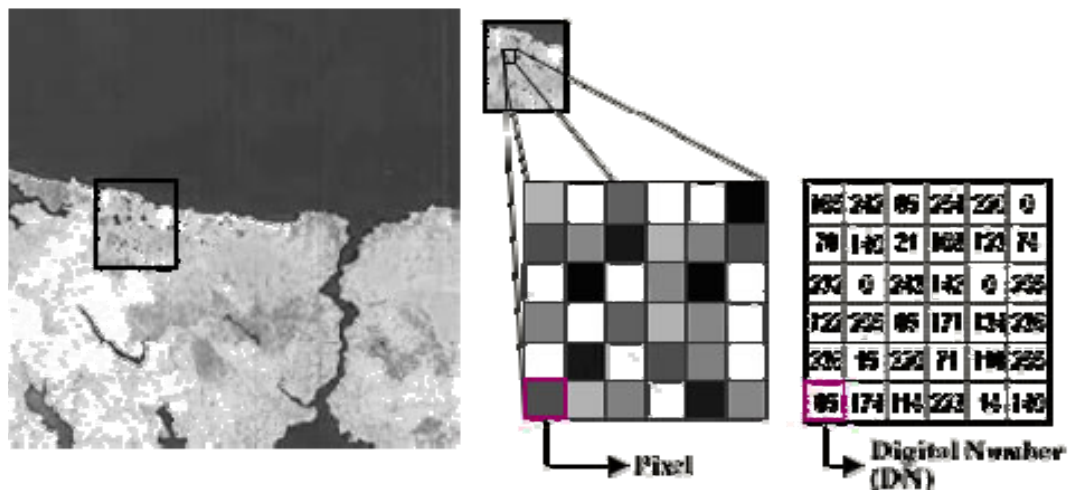
Figure 4.1 : Representation of a digital image

4.1 Image Resolution

Image resolution is defined as the ability of an imaging system to record fine details in a distinguishable manner [2]. Concept of resolution in optical and infrared remote sensing has to be examined at four different aspects as of Spatial, Spectral, Radiometric and Temporal resolutions. The analyst has to be familiar with these four types of resolutions in order to derive meaningful information.

4.1.1 Spatial Resolution

In a digital image, the pixel size limits the spatial resolution. The smallest resolvable object cannot be smaller than the pixel size. The pixel size is determined by the sampling distance. Spatial resolution refers to the size of the smallest object that can be resolved on the ground, thus is the smallest unit of an image and is measured by a pixel. The spatial resolution is defined by the distance on the ground that corresponds to a single pixel [17]. The spatial resolution of an imaging system is determined primarily by the Instantaneous Field of View, IFOV (Figure 4.2) of the sensor, which is a measure of the ground area viewed by a single detector element in a given instant in time. However this can often be degraded by other factors which introduce blurring of the image, such as improper focusing, atmospheric scattering and target motion [9].

10 m resolution   20 m resolution

40 m resolution   80 m resolution
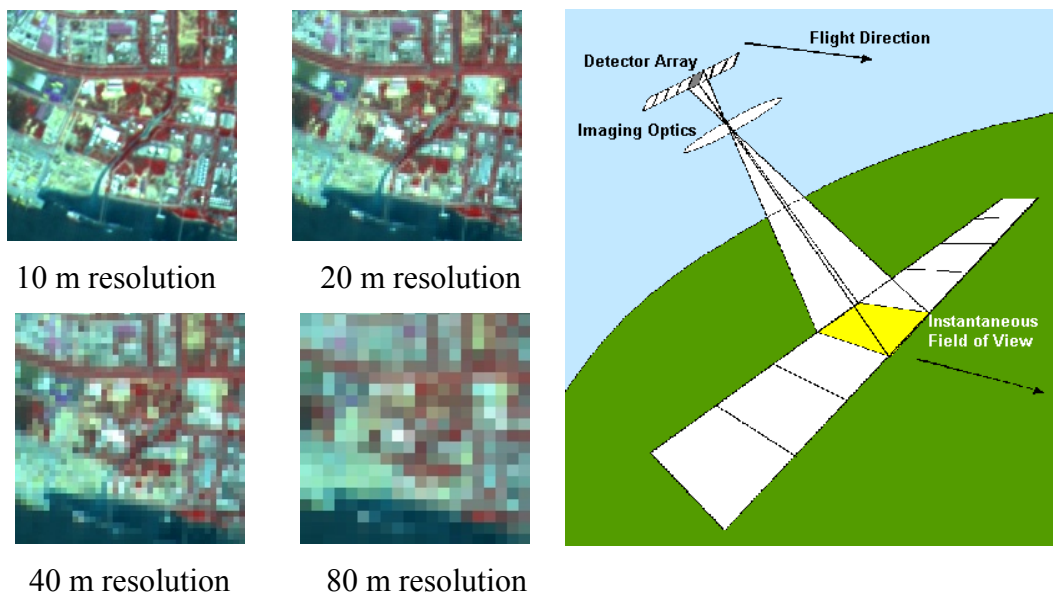
Figure 4.2 : Change in spatial resolutions due to Instantaneous Field of View

A spatial resolution of 10 meters means that an individual pixel represents an area on the ground of 10 meters by 10 meters. Thus any objects which are smaller than 10 meters will not be distinguishable in the image. A high spatial resolution such as 1 meter has been strongly demanded for agricultural applications where within field variability is studied. Low spatial resolution as 20 or 30 meters has limited the use of satellite imagery and encouraged the development of a new generation of land observation satellites to be launched (Figure 4.3) [17].
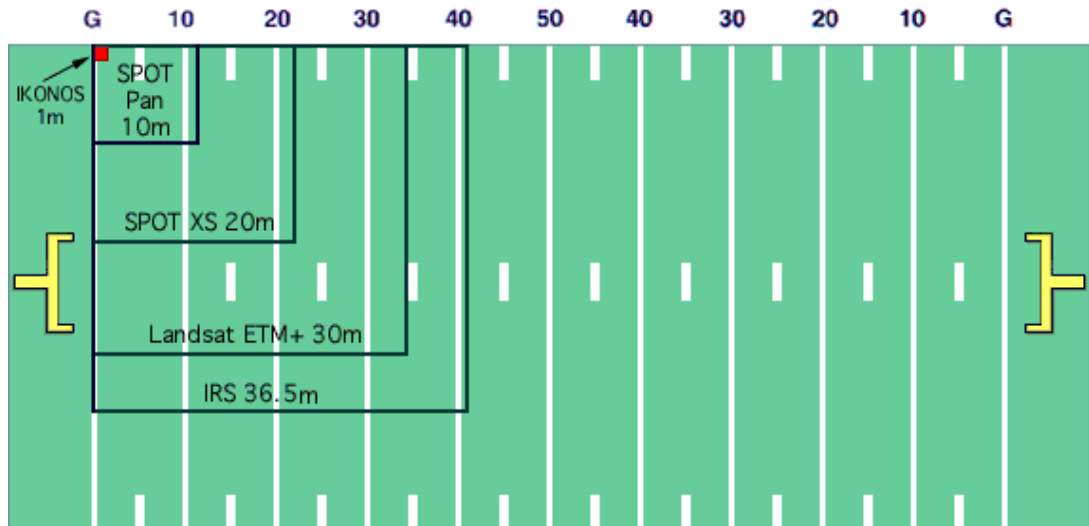
Figure 4.3 : Relative spatial resolutions of common sensors

4.1.2 Spectral Resolution

Spectral resolution refers to the wavelength intervals to which the sensor can detect. Sensors which can discriminate fine spectral differences are said to have a high spectral resolution in case of a sensor which can measure over a 0.05 um interval such as many hyperspectral systems has a fine spectral resolution. Detecting over a broad wavelength band of the electromagnetic spectrum such as a 35 mm camera using color film, has a coarse spectral resolution as the film records the entire visible spectrum [17]. Black and white film records wavelengths extending over much, or the entire visible portion of the electromagnetic spectrum. Its spectral resolution is fairly coarse, as the various wavelengths of the visible spectrum are not individually distinguished and the overall reflectance in the entire visible portion is recorded. Color film is also sensitive to the reflected energy over the visible portion of the spectrum, but has higher spectral resolution, as it is individually sensitive to the reflected energy at the blue, green, and red wavelengths of the spectrum (Figure 4.4).

Thus, it can represent features of various colors based on their reflectance in each of these distinct wavelength ranges.
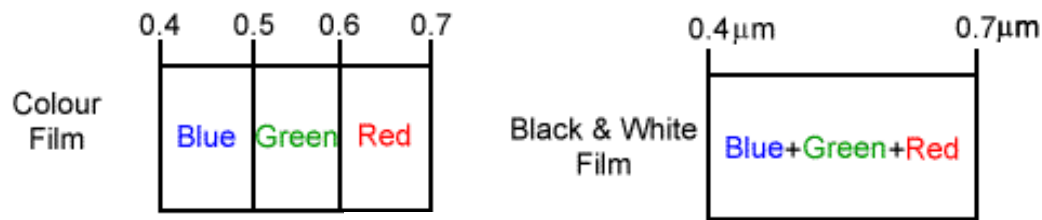
Figure 4.4 : Spectral resolutions of Colour and Black &White film compared

Many remote sensing systems record energy over several separate wavelength ranges at various spectral resolutions, being referred to as multi-spectral sensors. Advanced multi-spectral sensors called hyperspectral sensors, detect hundreds of very narrow spectral bands throughout the visible, near-infrared, and mid-infrared portions of the electromagnetic spectrum. Their very high spectral resolution facilitates fine discrimination between different targets based on their spectral response in each of the narrow bands [1].

4.1.3 Radiometric Resolution

Radiometric resolution is the number of data values associated with a pixel for each band of data detected. When describing the radiometric resolution of a sensor this is referred to as the number of bits into which the recorded data can be divided [17].

Imagery data are represented by positive digital numbers which vary from 0 to one less than a selected power of 2. This range corresponds to the number of bits used for coding numbers in binary format. Each bit records an exponent of power 2 so 1 bit is $2^1 = 2$. The maximum number of brightness levels available depends on the number of bits used in representing the energy recorded. Thus, if a sensor used 8 bits to record the data, there would be $2^8 = 256$ digital values available, ranging from 0 to 255. However, if only 4 bits were used, then only $2^4 = 16$ values ranging from 0 to 15 would be available. Thus, the radiometric resolution would be much less. Image data are generally displayed in a range of grey tones, with black representing a digital number of 0 and white representing the maximum value in case of 255 in 8-bit data. If a 2-bit image and an 8-bit image are to be compared (Figure 4.5), large difference in the level of detail discernible depending on the radiometric resolutions is observed [1].

While the arrangement of pixels describes the spatial structure of an image, the radiometric characteristics describe the actual information content in an image. Every time an image is acquired on film or by a sensor, its sensitivity to the magnitude of the electromagnetic energy determines the radiometric resolution. The radiometric resolution of an imaging system describes its ability to discriminate very slight differences in energy. Finer it is the radiometric resolution of a sensor; the more sensitive it is to detecting small differences in reflected or emitted energy.

<table>
<tr><td>(a)</td><td>(b)</td></tr>
</table>
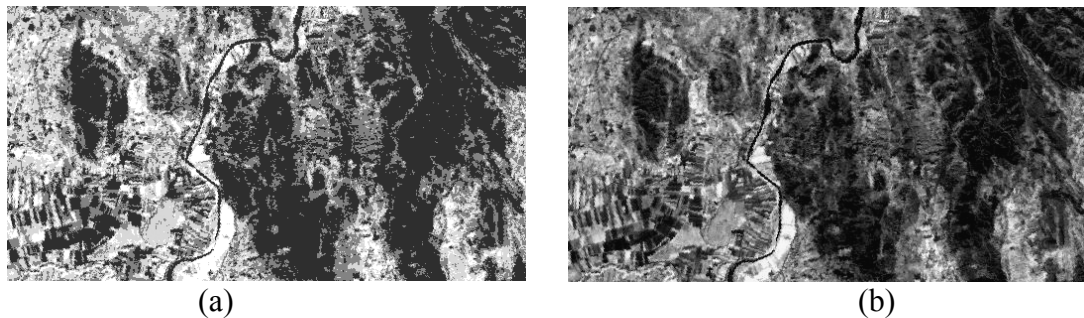
Figure 4.5 : Two images with different radiometric resolutions a) 2-bits b) 8-bits

4.1.4 Temporal Resolution

Temporal resolution is the frequency with which an image of a specific area or object can be acquired [17]. In addition to spatial, spectral, and radiometric resolution, the concept of temporal resolution is also important to consider in a remote sensing system. The concept of revisit period, which refers to the length of time it takes for a satellite to complete one entire orbit cycle, is the temporal resolution of the imaging system. The revisit period of a satellite sensor is usually several days, therefore the absolute temporal resolution of a remote sensing system to image the exact same area at the same viewing angle a second time is equal to this period. However, because of some degree of overlap in the imaging swaths of adjacent orbits for most satellites and the increase in this overlap with increasing latitude, some areas of the Earth tend to be re-imaged more frequently. Also, some satellite systems are able to point their sensors to image the same area between different satellite passes separated by periods from one to five days. Thus, the actual temporal resolution of a sensor depends on a variety of factors, including the sensor capabilities, the swath overlap, and latitude.

The ability to collect imagery of the same area of the Earth's surface at different periods of time is one of the most important elements for applying remote sensing data. Spectral characteristics of features may change over time and these changes can

be detected by collecting and comparing multi-temporal imagery. During the growing season, most species of vegetation are in a continual state of change and the ability to monitor those subtle changes using remote sensing is dependent on when and how frequently the imagery is collected. By imaging on a continuing basis at different times it is possible to monitor the changes that take place, whether naturally occurring in case of natural vegetation cover or flooding, or induced by humans such as urban development or deforestation. The time factor in imaging is important when:

- Persistent clouds offer limited clear views of the surface, especially in tropics

- Short-lived phenomena of floods, oil slicks, etc. need to be imaged

- Multi-temporal comparisons are required as in the spread of a forest diseases

- The changing appearance of a feature over time is needed to be distinguished from near-similar features in case of wheat and maize [1].

4.2 Pre-processing

Pre-processing operations, also known as image restoration and rectification, are applied to correct for sensor and platform specific radiometric and geometric distortions of data. Radiometric corrections may be necessary due to variations in scene illumination and viewing geometry, atmospheric conditions, and sensor noise and response. Each of these will vary depending on the specific sensor and platform used to acquire the data and the conditions during data acquisition. Also, it may be desirable to convert and/or calibrate the data to absolute radiation or reflectance units to make comparison possible between different data sources.

4.2.1 Radiometric Corrections

The reason for applying radiometric corrections is to reduce the influence of errors or inconsistencies in image brightness values; as referred to noise that may limit one's ability to interpret, process and analyze digital remotely sensed images. Radiometric noise generated by remote sensing instruments can take the form of random brightness deviations from electrical sources and coherent radiation interactions or more systematic variations that have spatial structure or temporal persistence. The

causes of radiometric noise are; changes in scene illumination, changes in atmospheric conditions, viewing geometry and instrument response characteristics.

Scattering occurs as energy passes through and interacts with the atmosphere. This reduces the intensity of the energy illuminating the surface. In addition, the atmosphere will further attenuate the signal reflecting from the target back to the sensor. Various methods of atmospheric correction can be applied ranging from detailed modeling of the atmospheric conditions during data acquisition, to simple calculations based solely on the image data. As a method, pixel brightness values are examined in an area of shadow or for a very dark object such as a large clear lake and the minimum value is determined. The correction is applied by subtracting the minimum observed value, determined for each specific band, from all pixel values in each respective band, since scattering is wavelength dependent. This method is based on the assumption that the reflectance from these features, if the atmosphere is clear, should be very small, if not zero. If we observe values much greater than zero, then they are considered to have resulted from atmospheric scattering [1].

For many quantitative applications of remote sensing data, it is necessary to convert the digital numbers to measurements in units which represent the actual reflectance or emittance from the surface. This is done based on detailed knowledge of the sensor response and the way in which the analog signal; the reflected or emitted radiation is converted to a digital number, called analog-to-digital (A-to-D) conversion. By solving this relationship in the reverse direction, the absolute radiance can be calculated for each pixel, so that comparisons can be accurately made over time and between images acquired with different sensors [1].

4.2.2 Geometric Corrections

All remote sensing imagery is inherently subject to geometric distortions. These distortions may be due to several factors, including: the perspective of the sensor optics; the motion of the scanning system; the motion of the platform; the platform altitude, attitude, and velocity; the terrain relief; and, the curvature and rotation of the Earth. Geometric corrections are intended to compensate for these distortions so that the geometric representation of the imagery will be as close as possible to the real world. Many of these variations are systematic or predictable in nature, and can be accounted for by accurate modeling of the sensor and platform motion and the

geometric relationship of the platform with the Earth. Other unsystematic, or random, errors cannot be modeled and corrected in this way. Therefore, geometric registration of the imagery to a known ground coordinate system must be performed [1].

Image-to-map registration process involves identifying the image coordinates of several clearly discernible points, called ground control points (GCPs), in the distorted image, and matching them to their true positions in ground coordinates such as latitude, longitude. The true ground coordinates are typically measured from a map, either in paper or digital format. Once several well-distributed GCP pairs have been identified, the coordinate information is processed by the computer to determine the proper transformation equations to apply to the original image coordinates to plot them into their new ground coordinates (Figure 4.6).
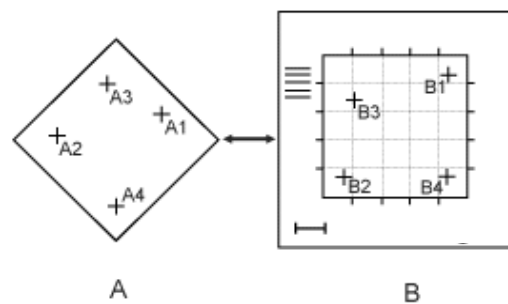
Figure 4.6 : Image-to-Map Registration scheme

Geometric registration may also be performed by registering one or more images to another image, which usually is already registered with a map. This is often done prior to performing various image transformation procedures. The procedure is similar to image-to-map registration. Instead of using geographical coordinates, ground control points on both the original and reference images are to be paired. Then the transformation equations are applied to the original image coordinates, registering it to the datum of the reference image [1].

In order to have a geometrically corrected image, a procedure called resampling is used to determine the digital values to place in the new pixel locations of the corrected output image. The resampling process calculates the new pixel values from the original digital pixel values in the uncorrected image. There are three common methods for resampling: nearest neighbor, bilinear interpolation, and cubic convolution [1].

Nearest neighbor resampling uses the digital value from the pixel in the original image which is nearest to the new pixel location in the corrected image (Figure 4.7a). This is the simplest method and does not alter the original values, but may result in some pixel values being duplicated while others are lost. This method also tends to result in a disjointed or blocky image appearance. Bilinear interpolation resampling takes a weighted average of four pixels in the original image nearest to the new pixel location. The averaging process alters the original pixel values and creates entirely new digital values in the output image (Figure 4.7b). This may be undesirable if further processing and analysis, such as classification based on spectral response, is to be done. If this is the case, resampling may best be done after the classification process. Cubic convolution resampling calculates a distance weighted average of a block of sixteen pixels from the original image which surround the new output pixel location (Figure 4.7c). As with bilinear interpolation, this method results in completely new pixel values. However, this method too produces images which have a much sharper appearance and avoids the blocky appearance of the nearest neighbor method [1].

(a) Nearest Neighbor (b) Bilinear Interpolation (c) Cubic Convolution
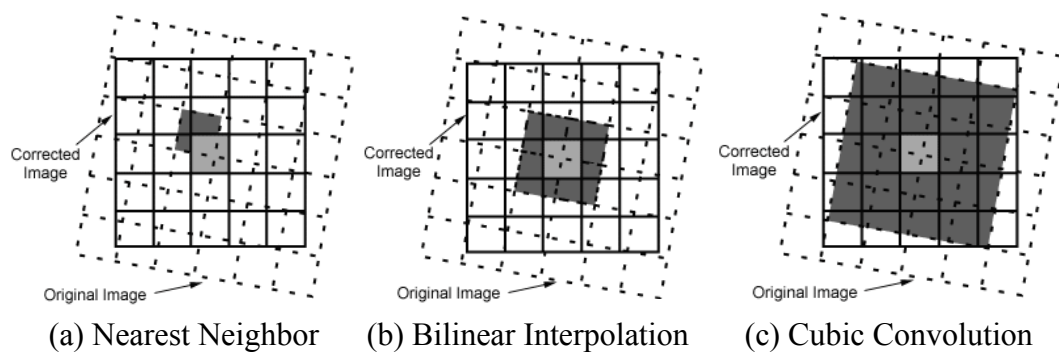
Figure 4.7 : Resampling Methods

4.3 Image Enhancement

Enhancements are used to make it easier for visual interpretation and understanding of imagery. The advantage of digital imagery is that it allows us to manipulate the digital pixel values in an image. Although radiometric corrections for illumination, atmospheric influences, and sensor characteristics may be done prior to distribution of data to the user, the image may still not be optimized for visual interpretation. Remote sensing devices, particularly those operated from satellite platforms, must be designed to cope with levels of target/background energy which are typical of all conditions likely to be encountered in routine use. With large variations in spectral

response from a diverse range of targets such as; forest, deserts, snowfields, water, no generic radiometric correction could optimally account for and display the optimum brightness range and contrast for all targets. Thus, for each application and each image, a custom adjustment of the range and distribution of brightness values is usually necessary.

In raw imagery, the useful data often populates only a small portion of the available range of digital values, commonly 8 bits or 256 levels. Contrast enhancement involves changing the original values so that more of the available range is used, thereby increasing the contrast between targets and their backgrounds. The key to understanding contrast enhancements is to understand the concept of an image histogram. A histogram is a graphical representation of the brightness values that comprise an image. The brightness values as 0-255 for 8 bit imagery, are displayed along the x-axis of the graph. The frequency of occurrence of each of these values in the image is shown on the y-axis. By manipulating the range of digital values in an image, graphically represented by its histogram, we can apply various enhancements to the data.

Linear contrast stretching involves identifying lower and upper bounds from the histogram; usually the minimum and maximum brightness values in the image, and applying a transformation to stretch this range to fill the full range (Figure 4.8a). A linear stretch uniformly expands this small range to cover the full range of values from 0 to 255. This enhances the contrast in the image with light toned areas appearing lighter and dark areas appearing darker, making visual interpretation much easier.

A uniform distribution of the input range of values across the full range may not always be an appropriate enhancement, particularly if the input range is not uniformly distributed. In this case, non-linear contrast stretching; also known as "Histogram equalization", is applied (Figure 4.8b). This stretch assigns more display values to the frequently occurring portions of the histogram. In this way, the detail in these areas will be better enhanced relative to those areas of the original histogram where values occur less frequently.

Spatial filtering is another set of digital processing functions which are used to enhance the appearance of an image. Spatial filters are designed to highlight or suppress specific features in an image based on their spatial frequency. Spatial

frequency is related to the concept of image texture. It refers to the frequency of the variations in tone that appear in an image. "Rough" textured areas of an image, where the changes in tone are abrupt over a small area, have high spatial frequencies, while "smooth" areas with little variation in tone over several pixels, have low spatial frequencies. Common filtering procedure involves moving a 'window' of a few pixels in dimension as 3x3 or 5x5 over each pixel in the image, applying a mathematical calculation using the pixel values under that window, and replacing the central pixel with the new value. The window is moved along in both the row and column dimensions one pixel at a time and the calculation is repeated until the entire image has been filtered and a new image has been generated (Figure 4.8c).

(a) Linear contrast stretching (b) Non-linear stretching (c) Convolution filtering
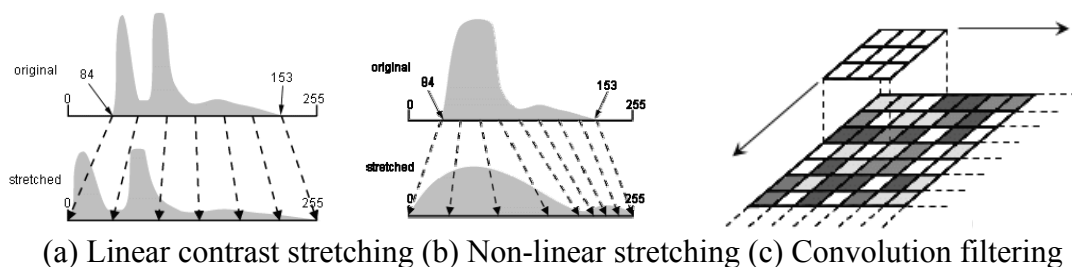
Figure 4.8 : Image enhancement techniques

By varying the calculation performed and the weightings of the individual pixels in the filter window, filters can be designed to enhance or suppress different types of features. Low-pass filter is designed to emphasize larger, homogeneous areas of similar tone and reduce the smaller detail in an image. Thus, low-pass filters generally serve to smooth the appearance of an image. Average and median filters, often used for radar imagery are examples of low-pass filters. High-pass filters do the opposite and serve to sharpen the appearance of fine detail in an image. One implementation of a high-pass filter first applies a low-pass filter to an image and then subtracts the result from the original, leaving behind only the high spatial frequency information. Directional, or edge detection filters are designed to highlight linear features, such as roads or field boundaries. These filters can also be designed to enhance features which are oriented in specific directions. These filters are useful in applications such as geology, for the detection of linear geologic structures.

4.3.1 Image Transformation

Image transformations typically involve the manipulation of multiple bands of data, whether from a single multispectral image or from two or more images of the same

area acquired at different times in case of multi-temporal image data. Either way, image transformations generate new images from two or more sources which highlight particular features or properties of interest, better than the original input images. Basic image transformations apply simple arithmetic operations to the image data.

A simple operation: "Band subtraction" is often used to identify changes that have occurred between images collected on different dates. Typically, two images which have been geometrically registered are used with the pixel values in one image being subtracted from the pixel values in the other. Scaling the resultant image by adding a constant; 127 in case of 8 bit imagery to the output values will result in a suitable difference image. In such an image, areas where there has been little or no change between the original images will have resultant brightness values around 127, mid-grey tones, while those areas where significant change has occurred will have values higher or lower than 127; brighter or darker depending on the direction of change in reflectance between the two images. This type of image transform can be useful for mapping changes in urban development around cities and for identifying areas where deforestation is occurring [1].

Band ratioing is one of the most common transforms applied to image data, serves to highlight subtle variations in the spectral responses of various surface covers. By ratioing the data from two different spectral bands, the resultant image enhances variations in the slopes of the spectral reflectance curves between the two different spectral ranges that may otherwise be masked by the pixel brightness variations in each of the bands. Most common uses of band ratioing are for calculating vegetation indices. Healthy vegetation reflects strongly in the near-infrared portion of the spectrum while absorbing strongly in the visible red. Other surface types, such as soil and water, show near equal reflectance in both the near-infrared and red portions. Thus, a ratio image of Landsat MSS Band 7, Near Infrared of 0.8 to 1.1 micrometers divided by Band 5 Red of 0.6 to 0.7 micrometers, would result in ratios much greater than 1.0 for vegetation, and ratios around 1.0 for soil and water resulting in enhancement of the discrimination of vegetation from other surface cover types. It is also better to identify areas of unhealthy or stressed vegetation, which show low near-infrared reflectance, as the ratios would be lower than for healthy green vegetation [1].

4.3.1.1 Difference Vegetation Index

One of the simplest vegetation index; the difference vegetation index (DVI) is sensitive to the amount of vegetation. Generally used for distinguishing soil and vegetation, but DVI doesn't deal with the difference between reflectance and radiance caused by the atmosphere or shadows, so it can't distinguish vegetation from soil in shady areas very well [1]. DVI is calculated as:

$$\text{DVI} = \text{NIR} - \text{Red} \qquad \qquad \textbf{(4.1)}$$

4.3.1.2 Ratio Vegetation Index

The simple ratio vegetation index (RVI), takes the ratio of the near infrared and red radiance. However, the RVI is affected by the 'noise' that is in the images due to factors such as atmospheric conditions. Typical ranges are a little more than 1 for bare soil to more than 20 for dense vegetation. A common practice in remote sensing is the use of band ratios to eliminate various albedo effects. Simple ratio vegetation index is calculated as:

$$\text{RVI} = \text{NIR} \,/\, \text{Red} \qquad \qquad \textbf{(4.2)}$$

4.3.1.3 Normalized Difference Vegetation Index

Most of the calculated values of ratio vegetation index will be quite small, but there will also commonly be some very large values. This makes it difficult to display properly without clipping the large values and stretching the remaining values over the available display range. Furthermore, the calculation is based on division so ratio vegetation index has a problem where red = 0, in this case using normalized difference vegetation index (NDVI) solves this problem [1].

NDVI is calculated as:

$$\text{NDVI} = (\text{NIR band - Red band}) \,/\, (\text{NIR band + Red band}) \qquad \textbf{(4.3)}$$

$$\text{NDVI} = (\text{NIR - VIS}) \,/\, (\text{NIR + VIS}) \ \ (\text{if no Red band exist} \qquad \textbf{(4.4)}$$

The differential reflectance in these bands provides a means of monitoring density and vigor of green vegetation growth using the spectral reflectivity of solar radiation. Chlorophylls, the pigments in green plants absorb light primarily from the red and blue portions of the spectrum, while a higher proportion of infrared is reflected or

scattered. NDVI tends to increase with increases in green leaf biomass or leaf area index. Rock and bare soil have similar reflectance in the red and the near infrared, so these surfaces will have values near zero. Green leaves commonly have larger reflectance in the near infrared than in the visible range. As the leaves come under water stress, become diseased or die, they become more yellow and reflect significantly less in the near infrared range. NDVI can be used as an indicator of relative biomass and greenness. If sufficient ground data is available, the NDVI can be used to calculate and predict primary production, dominant species, and grazing impact and stocking rates [18]. Green leaves have a reflectance of 20 percent or less in the 0.5 to 0.7 micron range; green to red, and about 60 percent in the 0.7 to 1.3-micron range (near infrared). The result is always between -1 and 1, in which -0.1 means not a green area and 0.6 is a very green area. However, dust and aerosols can cause errors; Rayleigh scattering, sub pixel-sized clouds. Near to these, large solar zenith angles and large scan angles increase red band with respect to near IR band and reduce the computed NDVI. So a preprocessing to decrease these effects is needed, but even after a preprocessing NDVI is still sensitive to external factors such as soil background that are most obvious in areas with sparse vegetation. Also NDVI is only sensitive to the green vegetation and might not recognize non-photosynthetic vegetation [1].

4.3.1.4 Perpendicular Vegetation Index

In calculating the perpendicular vegetation index (PVI) of a surface with vegetation, the reflectance in the red and NIR ranges are measured and plotted on a graph. The PVI is the perpendicular distance of the measured point from the soil line, defined as follows:

$$PVI = 1 / sqrt [(a^2+1) * (NIR - a * Red + b)] \qquad\qquad (4.5)$$

"b" and "a" are the slope and gradient of the soil line respectively. The PVI measures the changes from the bare soil reflectance caused by the vegetation. In this way it gives an indication of vegetative cover independent of the effects of the soil. PVI could be considered as a generalization of the DVI, which allows for soil lines of different slopes. PVI is quite sensitive to atmospheric variations, so comparing PVI values for data taken at different dates is risky. In order to do a comparison atmospheric correction is essential [1].

4.3.1.5 Enhanced Vegetation Index

Enhanced Vegetation Index (EVI) has similar algorithm with NDVI, but also it corrects some distortions in the reflected light caused by the particles in the air as well as the ground cover below the vegetation. Also when viewing areas with large amount of chlorophyll, EVI does not become saturated as easily as the NDVI. On the other hand EVI is unable to eliminate all obstacles. Clouds and aerosols can often block the satellite view of the surface entirely, glare from the sun can saturate certain pixels, and temporary malfunctions in the satellite instruments themselves can distort an image.

$$EVI = G * [(NIR - Red) / (NIR + C1*Red - C2*Blue + L)] \qquad \textbf{(4.6)}$$

Where r are atmospherically-corrected or partially atmosphere corrected (Rayleigh and ozone absorption) surface reflectance, L is the canopy background adjustment term, and C1, C2 are the coefficients of the aerosol resistance term, which uses the blue band to correct for aerosol influences in the red band. EVI, a product derived from the MODIS instrument, provides consistent spatial and temporal comparisons of global vegetation conditions used to monitor the Earth's terrestrial photosynthetic vegetation activity.

4.3.1.6 Transformed Vegetation Index

The Transformed Vegetation Index (TVI) attempts to eliminate negative values and convert NDVI histograms with a Poisson distribution to a Gaussian distribution by taking the square root of NDVI however it does not always accomplish the desired outcome as the result should be identical to the NDVI, some differences occur [1]. TVI is calculated as:

$$TVI = sqrt [(IR - red) / (IR + red)] \qquad \textbf{(4.7)}$$

4.4 Image Classification

Digital image classification is the method of using spectral information represented by the digital numbers in one or more spectral bands and classifying each individual pixel based on this spectral information. This type of classification is termed spectral pattern recognition. The objective is to assign all pixels in the image to particular

classes or themes. The resulting classified image is comprised of a mosaic of pixels, each of which belongs to a particular class, resembling a thematic map of the original image.

In case of image classification, information classes and spectral classes have to be clearly identified. Information classes are those categories of interest that the analyst is actually trying to identify in the imagery, such as different kinds of crops, different forest types or tree species, different geologic units or rock types. However, spectral classes are groups of pixels that are or near-similar with respect to their brightness values in the different spectral channels of the data. The objective is to match the spectral classes in the data to the information classes of interest [1]. Different landcover types in an image can be discriminated using some image classification algorithms using spectral features in each pixel. The image classification procedures are categorized as in two as supervised classification and unsupervised classification [9].

4.4.1 Supervised Classification

Supervised classification is the process where the analyst identifies homogeneous representative samples of the different surface cover types; training areas. The selection of appropriate training areas is based on the analyst's familiarity with the geographical area and their knowledge of the actual surface cover types present in the image. Thus, the analyst is supervising the categorization of a set of specific classes. The numerical information in all spectral bands for the pixels including these areas is used to train the computer to recognize spectrally similar areas for each class. Then a classification method of the analyst's choice such as parallelepiped, minimum distance, mahalanobis distance or maximum likelihood classification algorithm, is applied to determine the digital signatures present in the image for each training class. Once the signatures are located for each class, each pixel in the image is compared to these signatures and labeled to the class it most resembles digitally (Figure 4.9a). Thus in a supervised classification, information classes are first to be identified then used in the process of determining the spectral classes which represent them [19].

4.4.2 Unsupervised Classification

Unsupervised classification in a sense is the inverse of supervised classification process. Spectral classes are grouped first, based solely on the digital likeliness of the information in the data, and are then labeled by the analyst to generate information classes (Figure 4.9b). Clustering algorithms such as ISODATA or k-means method are used to determine the statistical groupings or structures in the data. Usually, the analyst specifies how many groups or clusters are to be looked for in the data. In addition to specifying the desired number of classes, the analyst may also specify parameters related to the separation distance among the clusters and the variation within each cluster. The final result of this iterative clustering process may result in some clusters that the analyst will want to subsequently combine, or clusters that should be broken down further - each of these requiring a further application of the clustering algorithm. Thus, unsupervised classification is not completely without human intervention. However, it does not start with a pre-determined set of classes as in a supervised classification [19].

(a) Supervised Classification   (b) Unsupervised classification
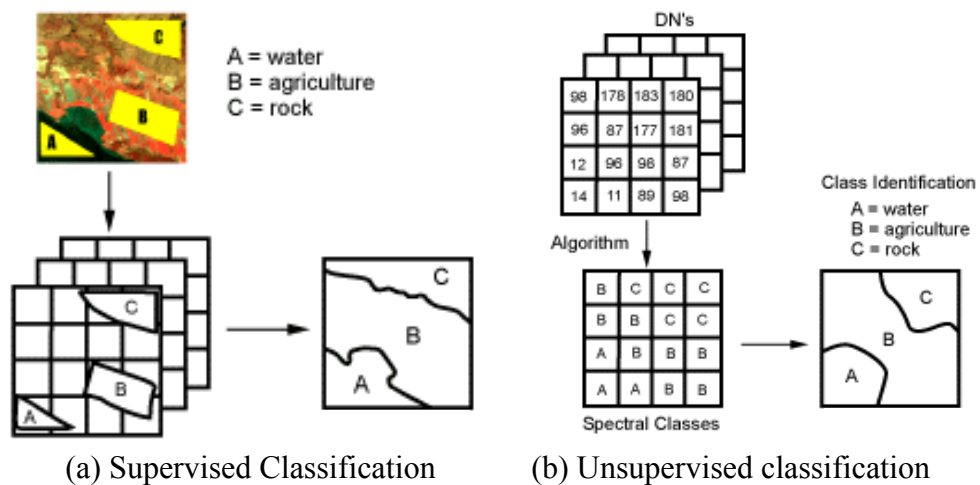
Figure 4.9 : Image Classification methods

4.4.3 Classification Accuracy

A most common and typical method used by researchers to assess classification accuracy is with the use of an error matrix also known as confusion matrix or contingency table (Table 4.1). An error matrix is a square assortment of numbers defined in rows and columns that represent the number of sample units as pixels, clusters of pixels, or polygons, relative to the their actual sources as confirmed on the ground. As the result, percentages of overall classification accuracy, omission and

commission error by category are to be computed. These values are derived based on a sample ground truth data. A Reference pixel is a point on the classified image for which actual data it resembles is known. Reference pixels are randomly selected based on available sources of land cover reference information, such as existing maps, aerial photos or in-stu examinations. An accurate assessment can be made only if these sources are chosen independently of those used in the process of classification [20].

Error of omission is the percentage of pixels that should have been clustered into the specified class but were not. Errors of omission are also expressed as the producer's accuracy. Producer's accuracy represents the percentage of a given class that is correctly clustered pixels with respect to the reference pixels (Table 4.1). It is calculated by dividing the number of correctly clustered pixels by the total number of reference pixels for that class. Error of commission reveals pixels that were assigned to a given class when they actually belong to another. Errors of commission are also expressed as the user's accuracy. User's accuracy represents the probability that a given pixel will appear on the ground as it is classed. It is calculated by dividing the number of correctly clustered pixels; derived from the reference pixels, by the total number of pixels in that class (Table 4.1). An important factor in determining the accuracy of a classification is the number of reference pixels used [20].

Table 4.1: Example of an error matrix

Classified Data	Ground Reference Data				
	Class 1	Class 2	Class 3	Total Pixels (classified)	User's Accuracy
Class 1	n1	n2	n3	n1+n2+n3	n1 / (n1+n2+n3)
Class 2	n4	n5	n6	n4+n5+n6	n5 / (n4+n5+n6)
Class 3	n7	n8	n9	n7+n8+n9	n9 / (n7+n8+n9)
Total Pixels (Reference)	n1+n4+n7	n2+n5+n8	n3+n6+n9	∑ n(1,9)	
Producer's Accuracy	n1 / (n1+n4+n7)	n5 / (n2+n5+n8)	n9 / (n3+n6+n9)		(n1+n5+n9) / ∑ n(1,9)

5. WILDFIRE MONITORING AND ASSESSMENT

5.1 Properties of Wildfires

A wildfire is any uncontrolled fire of flammable vegetation that occur in the countryside or a wilderness area, differing from other fires by its extensive size, the speed at which it can spread out from its source of origin, its potential to change direction unexpectedly, and its ability to jump gaps such as roads, rivers and fire breaks [22]. Wildfires occur on every continent except Antarctica. Fossil records and human history point out instances of wildfires in periodic intervals. Causing damage both to property and human life, wildfires may sometimes have beneficial effects on such as some plant species being depend on the aftereffects of a wildfire for growth and reproduction [23]. Wildfires are mainly characterized by their cause of ignition and physical properties such as direction and speed of propagation as well as type of combustion [22].

5.1.1 Cause of Ignition

Wildfires set off for either natural or human induced reasons. Natural fires are commonly caused by lightning events, and not as often by combustion of dry fuel such as sawdust or dry vegetation, where as human induced fires are due to any number of reasons, some of which include careless smoking, improperly extinguishing campfires, urban recreation and arson [24]. Weather conditions have direct effect to the occurrence of wildfires as in lightning strikes, or indirect effect such as by an extended lack of moisture or drought that increases the availability of fuel. Lightning strikes the Earth over 100,000 times a day and of these, 10-20% causes a fire. Besides the lighting, accumulation of dead grass, leaves and twigs in a pile are sometimes likely to create heat, enough to spontaneously combust and ignite the surrounding area [25].

Three elements, referred as "The Fire Triangle" need to be present simultaneously in order for a wildfire to initiate: Fuel, oxygen, and heat source. Fuel is any flammable material surrounding a fire, either organic such as trees, grass, and brush or inorganic

such as urban residences. Larger the present fuel load, more intense is the fire. The oxygen is supplied by the air and the heat sources increases the temperature of the fuel high enough to ignite. As well as human sources, natural phenomenon such as lightning strikes, hot currents, and even the sun can all provide sufficient heat to spark a wildfire [26]. Thus, without all three of these elements, the fire goes out. Furthermore, the fire propagates in the direction of the most abundant supply of these three elements, while its rate of combustion is limited by the least abundant element. Thus wildfires occur when all of the necessary elements of a fire triangle come together: An ignition source is brought into contact with a combustible material in this case the forest; that is subjected to sufficient heat and has an adequate supply of oxygen from the ambient air.

High moisture content usually prevents ignition and slows propagation, since higher temperatures are required to evaporate any water within the fuel and heat it to its fire point [27]. Dense forests provide more shade, lowering the ambient temperature and increasing the humidity, therefore are less susceptible to wildfires. Less dense vegetation such as grass and leaves are easier to ignite, containing less water than denser material such as branches and trunks [28]. Vegetation continuously loose water by evapotranspiration, however lost water is usually balanced by absorption from the soil, humidity, or rain. When this balance is not sustained, the vegetation dries out and becomes more flammable, often as a consequence of droughts [29].

5.1.2 Physical Properties

The direction of propagation depends on the fronts of the wildfire. A wildfire front (Figure 5.1) is the portion supporting continuous flaming combustion, where unburned trees meet active flames, or the smoldering transition between unburned and burned vegetation [30].
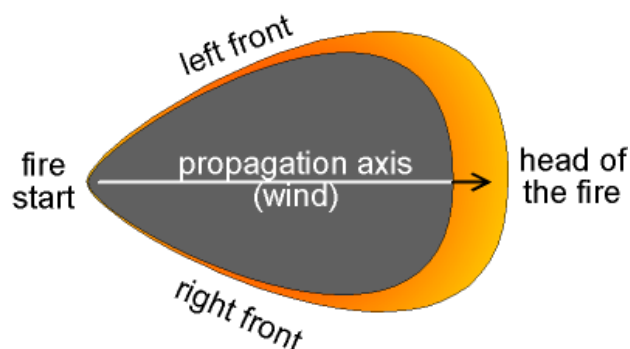

Figure 5.1 : Physical model of a wildfire

As the front approaches, the both the surrounding air and vegetation are heated through convection and thermal radiation. Initially, exposed wood dries as water is vaporized at a temperature of 100 °C. Next, the pyrolysis of wood at 230 °C releases flammable gases. Finally, wood smolders at 380 °C and when heated sufficiently, ignite at 590 °C. Even before the flames of a wildfire arrive at a particular location, heat transfer from the wildfire front warms the air to 800 °C, which pre-heats and dries flammable materials, causing materials to ignite faster and allowing the fire to spread faster [31]. The speed of propagation depends on the density of the forest and the weather parameters. Wildfires have a Rapid Forward Rate of Spread (FROS) when burning through dense, uninterrupted fuels. They can move as fast as 10.8 kilometers per hour in forests and 22 kilometers per hour in grasslands [32].

5.1.3 Fire Classifications

Fires are classified according to their combustion stage as smoldering fire, flaming combustion and glowing combustion. Smoldering fire is the type that emits smoke but no flame and is rarely self sustained. A fire is classified as flaming combustion when flames are present. With this type of fire, charcoal can be produced in the absence of oxygen. Glowing combustion is a later stage of the fire and is characterized by a slower rate of combustion and blue flame.

Fires are also classified according to their target fuel. Three types of fires occur in forested areas depending on fuel and conditions: Ground fire, surface fire, and crown fire. Ground fires occur on the ground, often below the leaves where as surface fires occur on the surface of the forest up to 1.3 meters high. Crown fires however are the most dangerous fire type and spread the fastest. Crown fires occur in the top region of the trunks and the canopy of the trees, depending upon the surface fires to reach the crowns. This type of fire is the most destructive and, independent where flames easily spread from canopy to canopy [24].

5.1.3.1 Ground Fires

Ground fires smolder or slither slowly through the litter and humus layers, consuming all or most of the organic cover, and exposing mineral soil or underlying (Figure 5.2). These fires occur as the result of prolonged droughts when the entire soil organic layer is dried sufficiently. Ground fires may burn for weeks or months

until precipitation and low temperatures extinguish the fire, or until the fuel runs out. [33]

Figure 5.2 : Example of a ground fire

5.1.3.2 Surface Fires

Surface fires burn the upper litter layer and small branches that lie on or near the ground from the top of the forest floor to about 3 meters above ground. Surface fires usually move rapidly through an area, and do not consume the entire organic layer (Figure 5.3). Moisture often prevents ignition of the humus layer, and protects the soil and soil-inhabiting organisms from the harm. If the fire is persistent and is strong enough, the heat pulse generated at the fronts damages tissues underneath the thick bark of large trees, girdling the root collars and shrubs, reducing small diameter branches and fine surface fuels. [33]

Figure 5.3 : Example of a surface fire

5.1.3.3 Crown Fires

Crown fires occur when surface or ground fires become strong enough to engulf the tree crowns in flames, spreading rapidly to nearby crowns (Figure 5.4). Crown fires are most likely to happen in forests during periods of drought and low relative humidity; particularly in areas with heavy accumulations of understory material called ladder fuels such fallen trees, logging slash and combustible understory vegetation. Crown fires generate remarkable heat which rises in a strong vertical convection, causing the fast surface winds to fan the flames even more. Heated air blowing across the flames also warms and dries the fuels ahead of the fire, causing the vegetation ahead of the flaming front to release flammable gases. Similar to ground fires, crown fires kill all effected trees and shrubs in their path, consume the surface organic layers and only end if runes out of fuel or precipitation cools the fire and wets the fuels sufficiently to inhibit burning [33].

Figure 5.4 : Example of a crown fire

5.2 Detection of Wildfires

Fast and effective detection is one of the key factors in wildfire management. Early detection methods were focused on early response, accurate results in both daytime and nighttime and the ability to prioritize threat. Fire lookout towers were used in the early 20th century and fires were reported using telephones, carrier pigeons, and heliographs [34]. Aerial and land photography using instant cameras were used in the 1950s until infrared scanning was developed for fire detection in the 1960s. However, information analysis and delivery was often delayed by limitations in

communication technology. Early fire analyses were hand-drawn on maps at a remote site and sent via overnight mail to the fire manager [35].

Currently, public hotlines, fire lookouts in towers, and ground and aerial patrols are used as means of fire detection. High risk areas that feature thick vegetation, a strong human presence, or are close to an urban area are monitored using ground sensor networks. Detection systems include wireless sensor networks working as automated weather systems to detect temperature, humidity, and presence of smoke [36]. These may be battery-powered, solar-powered, or tree-rechargeable which is ability to recharge the battery system by means of small electrical currents in vegetation [37]. Medium risk areas are monitored by scanning towers that incorporate fixed cameras and sensors to detect smoke or infrared signature of carbon dioxide produced by fires. Capabilities such as night vision, brightness detection, and color change detection may also be integrated with sensor arrays [38]

5.3 Wildfire Assessment and Analysis

In order to assess the outcome of a geographic event, the information derived from data acquired by means of satellite technology such as remote sensing have to be integrated within a location based system for analysis and query. Geographic Information Systems (GIS) is a location based information system which incorporates geographical features with tabular data in order to map, analyze, and assess any geographical issue. The data in a GIS is spatially referenced to locations on the earth, coupled with a tabular data named as attribute data, the information about each of the spatial features. The affiliation of these data types enables GIS to be an effective problem solving tool through spatial analysis [39]. When specifically designed for wildfires, a GIS would provide information about forest, soil and meteorological conditions as well as transportation and logistic information in order to determine risk areas and develop early response schemes and effective extinguishing plans. Post fire damage assessment can be performed and forest rehabilitation can be modeled with respect to topography and soil prosperities. Remote sensing systems employing multispectral and infrared sensors to identify and target wildfires are the key to provide such data. Satellite images obtained from remote sensing systems which provide synoptic view and are sufficient to monitor very large fire areas, can be used as layers in a GIS; either directly or processed to

extract specific information to aid the assessment and analysis of wildfires. Moderate resolution multispectral satellites such as Landsat TM and SPOT offer multispectral images from 30 meters up to 10 meters spatial resolution. Sensors such as Advanced Along Track Scanning Radiometer in Envisat and Along Track Scanning Radiometer in ERS measures infrared radiation emitted by fires, identifying hot spots greater than 39 °C [40].

5.3.1 Global State of Affairs

GIS is one of the most effective tools for wild fire monitoring and assessment providing the core infrastructure to create a forest information system. In term of wildfire assessment, GIS provides a useful base for information such as geographical, geological, and meteorological and forestry data to be cross evaluated. Canadian Forest Fire Behavior Prediction (FBP) System is an example of GIS integration in order to estimate d fire spread rate, fuel consumption, and fire intensity as well as providing fire descriptions [41]. Switzerland uses GIS to achieve an operational forest fire management system of the Swiss National Park to provide an interactive decision support system, which enables the training of the people in charge with a fire simulator and the prediction of the damage potential [42]. Remote sensing systems are also used effectively to detect, monitor and evaluate wildfires around the world. Multispectral images are especially useful for pre and post fire evaluations such as estimating above ground biomass for different forest types of fire susceptible regions [43], detecting change in forest types subsequent to wildfires [44] and characterization of forest recovery [45]. The National Oceanic and Atmospheric Administration's (NOAA) Hazard Mapping System combines remote sensing data from satellite sources such as Geostationary Operational Environmental Satellite (GOES), Moderate-Resolution Imaging Spectroradiometer (MODIS), and Advanced Very High Resolution Radiometer (AVHRR) for detection of fire and smoke plume locations [46]. Remote sensing and GIS can also be integrated in order to provide powerful pre and post fire assessment tools as in a study in Germany for improvement of a forest GIS by integration of remote sensing data for the observation and inventory of protective forests in the Bavarian Alps [47] and a study in China to analyze forest potential fire environment based on GIS and remote sensing [48].

51

5.3.2 Current Situation in Turkey

Turkey has 21.2 million ha of forestland, of which 12 million ha being susceptible to fires, mostly at regions where Mediterranean climate is dominant with high temperatures and almost no precipitation. From 1937 to 2007; 82556 fires burned a total of 1582590 hectares of forest land with an average area burned per fire of 19.17 ha consuming the forest land annually resulting in high suppression costs and loss in economy, ecology and even human life [49].

GIS being a newly developing technology, is rather appealing in terms of forestry applications in Turkey. In years of 1998 and 2001, GIS was used to integrate the local cadastre data with forest management plans for the first time in Karabük Forest Management Directorate. Later in 2004, all local forest management data were processed within a GIS alongside digitized the forest transportation maps. Early in 2007, a Forest Fire Management System based on ArcGIS and Oracle database software was initiated for assembling fire reports and tracking the fire trucks. Later in 2008 the system was developed to carry out early fire detection by integrating with ground sensors as well as performing statistical queries such as shortest distance / fastest time, fire propagation modeling, fire potential and probability with respect to fuel properties, and burned area detection from layers including remote sensing data, forest structure, administrative borders, local temperature, precipitation and detailed distribution of individual tree types [50].

Besides the forest fire management system; a Permission Information System to query any legal permission regarding forestlands and a Biodiversity Monitoring System to gather and extract information about forest ecology, especially in fire-affected zones are being developed. Furthermore, post fire studies to rehabilitate the burned forest with fire resistant silviculture are being planned again using a GIS [50].

6. APPLICATION

Forests, as well as being one of the exceptionally valued natural resources due to their rich content of wood stock and industrial raw materials; have the upmost importance through out the ecologic process by regulating the precipitation and underground waters, counteracting the erosion and balancing the oxygen – carbon dioxide proportions thus preserving the atmosphere chemistry and the carbon cycle [23]. Along the Mediterranean and southern Aegean regions of Turkey especially during July and August, high temperature combined with low humidity poses a grave danger for forest terrain in terms of wildfires. Moreover, the statistics verify that vast majority of the forest fires are human induced due to increasing demand for land. Whether the cause of fire is natural or intentional, the damage is rapid and should be monitored by newly developing satellite technology in stages of before, during and after. Remote sensing, having a significant place in hazard monitoring and evaluation; is able to provide – instantly if available – images of the fire zone in visible and infrared spectrums by multispectral satellites having mid or high spatial resolution. By means of comparing the post fire image with the pre fire images of the zone, the quantitative and the qualitative analysis of the damage in vegetation can be done rapidly and precisely.

6.1 Study Area and Data Used

The objective of this study is to analyze the forest fire that took place between July 31st and August 5th, 2008 effective at Antalya province, Manavgat and Serik municipalities. Serik municipality, having approximately 26 m altitude and 22 km of coastline; lies 38 km east of Antalya (Figure 6.1). Spread over 1,550 km² of rough plains, the municipality contains 65,764 hectares of forest terrain. [52]. 5 km east of Serik is Manavgat municipality, having agricultural fields from the coastline to the Taurus Mountains. 72% of the acreage (165,584 hectares) consists of forest and brushwood, where southern skirts of the Taurus Mountains are covered with red pine (*Pinus brutia*). As the altitude increases, red pine leaves its place to black pine (*Pinus nigra*), spruce, cedar and juniper [53].

53

Figure 6.1 : The map of the study area

Both municipalities are under the effect of Mediterranean climate where winters are warm and rainy; summers though are hot and arid. The highest temperature is measured on July 2002 as 41.0 C°. Annual precipitation is about 945.6 kg/m² [53].

Through out this study, multispectral SPOT 4 HRVIR data set with level 2A preprocessing acquired on August 7th, subsequent to fire (Figure 6.2a) is used. The data set consist of 4 spectral bands (Green: 0.5-0.59µm, red: 0.61-0.68µm, near infrared: 0.79-0.89µm and shortwave infrared: 1.53-1.75µm) each having 8 bit radiometric and 20 meter spatial resolution. In order to analyze the satellite image with additional data, six topographic maps in 1:25,000 scale are integrated and used as geographic references (Figure 6.2b). Ikonos images having 1 meter spatial resolution from Google Earth and areal photographs of the fire zone taken from a helicopter are used as ancillary data through out assessment procedure.

(a)   (b)
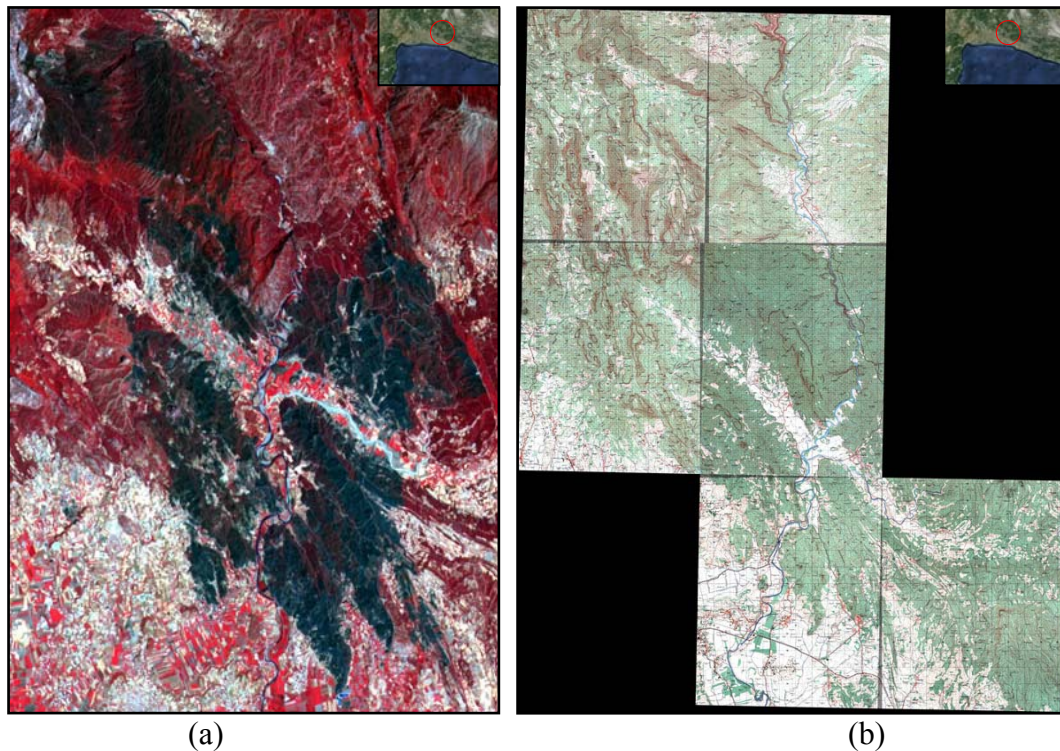
Figure 6.2 : Data used in the study

a) SPOT 4 Image after fire: August 7th, 2008 (RGB: Near IR, Green, Blue)
b) 1:25,000 scaled digital topographic maps of the fire zone

6.2 Methodology

In this study, pixel based multispectral image classification techniques were applied to the post fire image in order to extract the burned and partially damaged forest areas due to the forest fire that took place in Antalya province to be compared with local forest management data and analyzed within a geographical information system. The image was preprocessed as level 2A meaning that radiometric correction for distortions due to differences in sensitivity of the elementary detectors of the viewing instrument is applied and geometrical correction is done in a UTM WGS84 cartographic projection without being tied to ground control points [54]. The methodology in order to determine and analyze the burned area is in Figure 6.3.
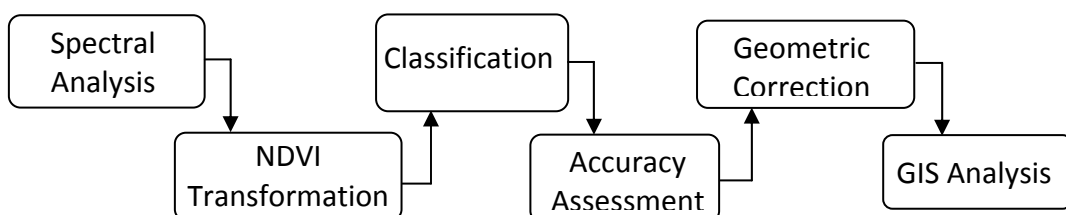
Figure 6.3 : Methodology

6.3 Spectral Analysis

The difference in reflectance of the electromagnetic energy containing various wavelengths enables the objects to be differentiated with respect to their spectral features. The variation of reflectance at near infrared and visible spectrums is the key to identify the diversity and quality of the vegetation. If the reflectance is high at the near infrared portion whereas low at the visible portion, then the area corresponding to such pixels is to contain dense vegetation, most likely forest. Same situation is valid for the health of the vegetation. In other words, the difference between near infrared and visible spectrum is high for healthy vegetation whereas for damaged vegetation, this difference is quite low (Figure 6.4).

(a)   (b)
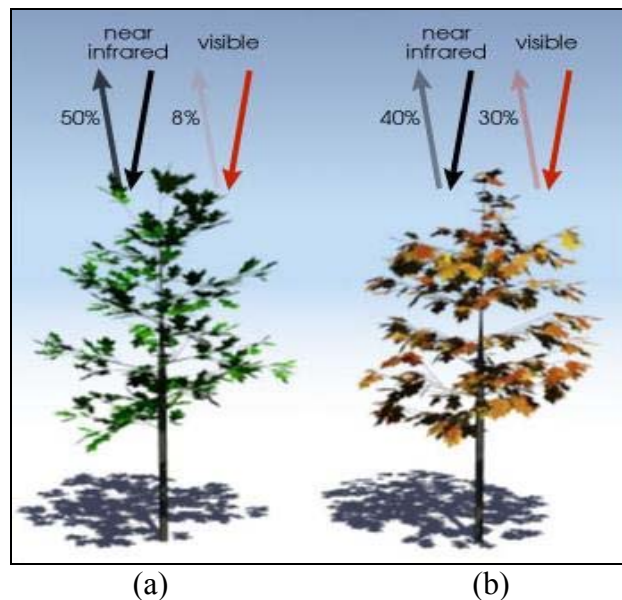
Figure 6.4 : Visible and NIR reflectance in a) healthy b) stressed vegetation

When the post fire image acquired on August 7th is examined, severely damaged but alive vegetation is detected within the boundaries of the fire. When compared to healthy forest's spectral reflectance, these regions have quite low reflection at near infrared wavelength. However, burned regions have the common reflectance pattern of near infrared reflection being lower than the reflection at visible spectrum, indicating no sign of biomass (Figure 6.5).
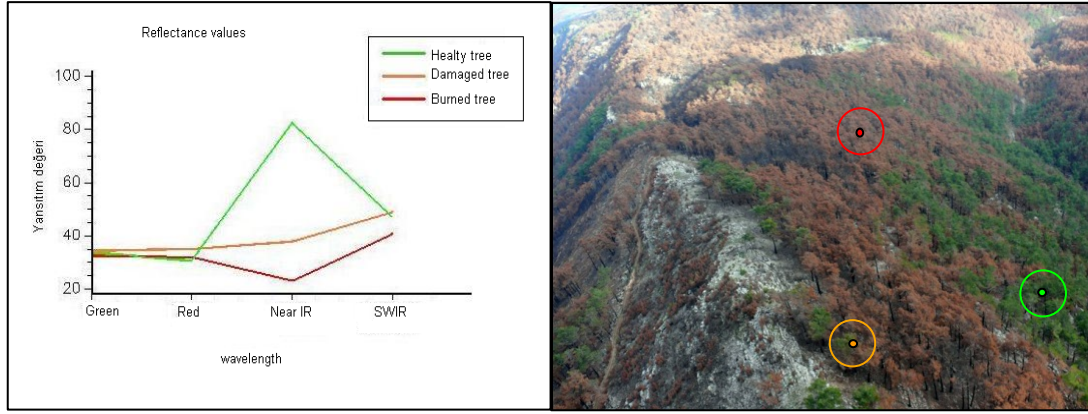
Figure 6.5 : Spectral signature samples of healthy, damaged and dead forest

6.3.1 NDVI Transformation

Normalized Difference Vegetation Index transformation, an effective process to emphasize the variations in vegetation biomass; relies on taking the ratio of difference between reflectance at near infrared and red wavelengths to the sum of their reflectance [18]. Pixel values end up between -1 and 1 after the NDVI transformation where low values (0.1 or lower) correspond to unvegetated terrain such as bare soil, rock or snow, mid values (between 0.2 – 0.3) correspond to shrubs and grasslands and high values (0.3 and higher) are likely to be dense vegetation such as forests of various density [55].

In this study, NDVI transformation was applied to the post fire image in order to increase the accuracy of further classification of the burned forest (Figure 6.6). Outcome values for burned forest regions were found to be between -0.28 and -0.05, damaged but alive regions were between 0.02 and 0.29, healthy regions were between 0.3 and 0.5. The NDVI image was then added to the post-fire image data set as the 5th band, thus damaged but alive forest regions with low reflection at near infrared wavelength was expected to be classified more accurately.
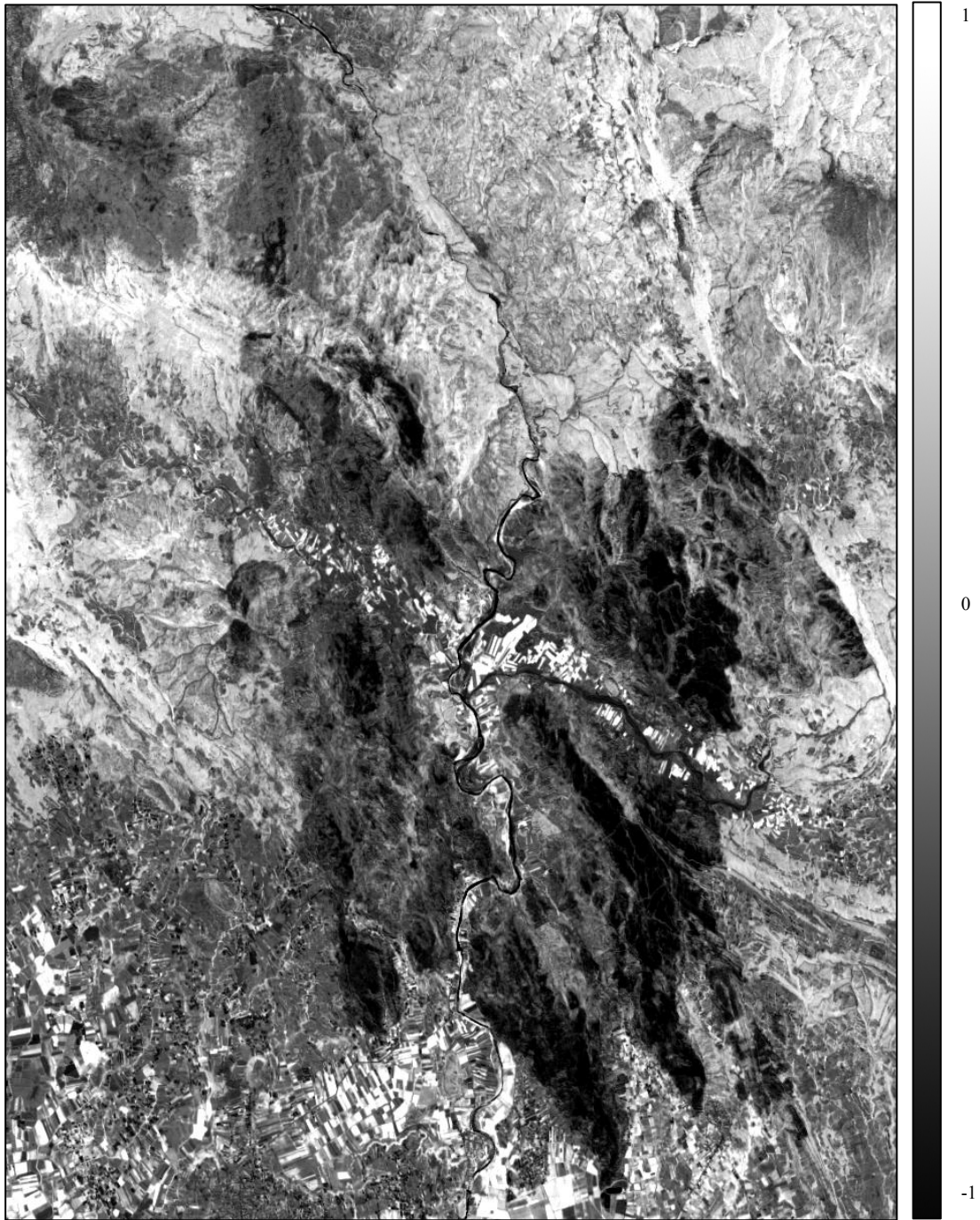
Figure 6.6 : NDVI transformation applied to post fire image

6.4 Classification

In order to determine and distinguish the burned and damaged forest, supervised and unsupervised pixel based multispectral classification methods were applied on post fire image data set acquired on August 7th 2008 including the NDVI band.

6.4.1 Supervised Classification

Maximum likelihood algorithm was used in order to perform supervised classification. The algorithm is based on a statistical decision rule that examines the probability function of a pixel for each of the classes, and assigns the pixel to the class with the highest probability. The classifier assumes that the training statistics for each class have a Gaussian normal distribution and then uses the training statistics to compute a probability value of whether it belongs to a particular land cover category class [56].

During the supervised classification process, 7 training classes with a total of 66671 homogeneously scattered pixels were defined using IKONOS satellite image with 1 meter spatial resolution as ground truth data (Figure 6.7). Maximum Likelihood algorithm was then applied as the classifier, resulting with 7 information classes which are burned, damaged and dense forest, water, coarse vegetation, bare soil and other (Figure 6.8).
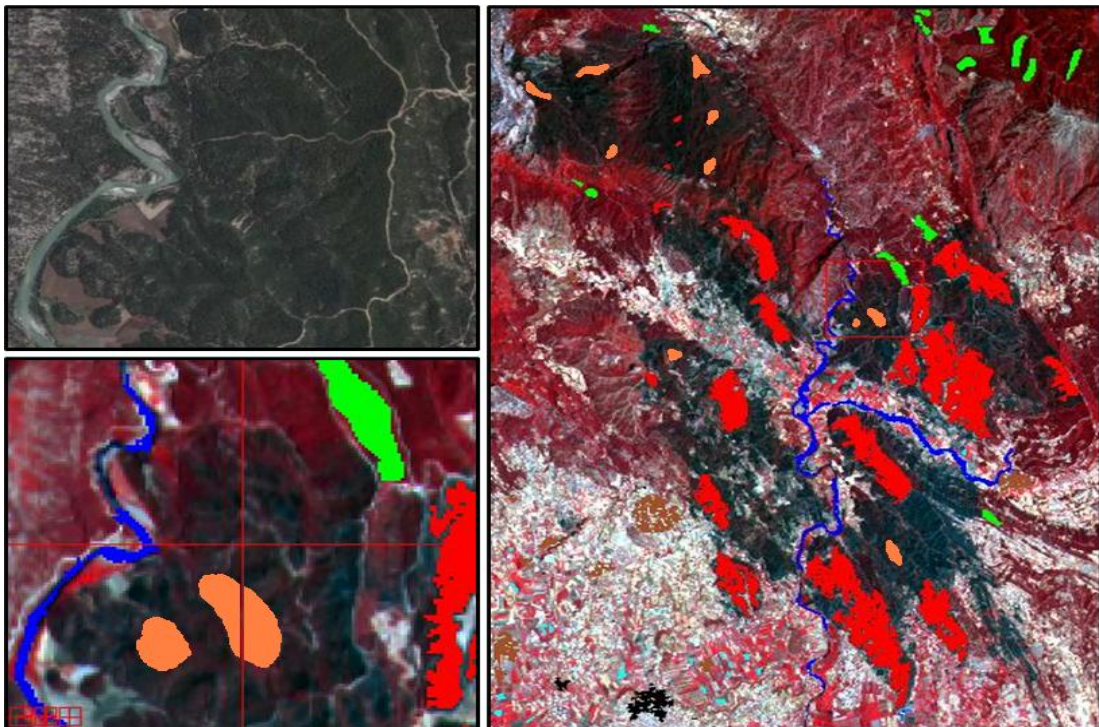
Figure 6.7 : Training area selection for supervised classification
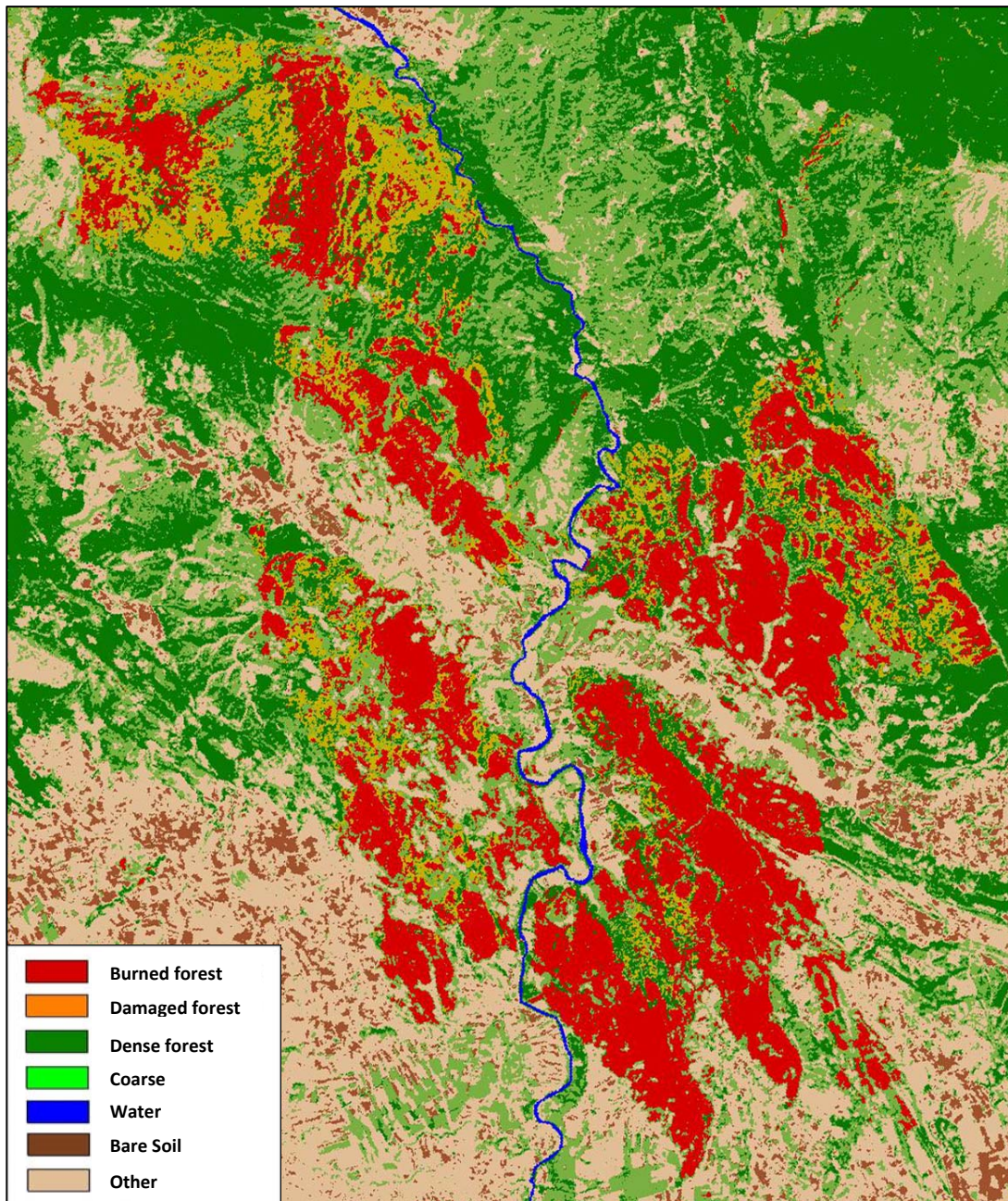
Figure 6.8 : Supervised classification result

6.4.2 Unsupervised Classification

Iterative Self-Organizing Data Analysis (ISODATA) technique was used for unsupervised classification of the post fire image. The ISODATA classification algorithm is an iterative procedure, assigning first an arbitrary initial cluster vector. The second step classifies each pixel to the closest cluster. In the third step the new cluster mean vectors are calculated based on all the pixels in one cluster. The second and third steps are repeated until the "change" between the iteration is below the user defined threshold. The threshold is defined either by measuring the distances the mean cluster vector have changed from one iteration to another or by the percentage of pixels that have changed between iterations [57].

Throughout the unsupervised classification procedure, post fire image is first segmented into 25 spectral clusters with a threshold value of 1% change in 100 iterations. Then clusters with similar reflectance properties are analyzed (Figure 6.9) and manually merged into 14 information classes which are burned, damaged and 6 different healthy forest classes varied by vegetation density, water, coarse vegetation, cultivated fields, bare fields, bare soil and other soil (Figure 6.10).

Figure 6.9 : Cluster analysis and merging

Figure 6.10 : Unsupervised classification result

6.5 Accuracy Assessment

Accuracy assessment for the classification results were performed using an error matrix developed by comparing randomly and independently selected test pixels with the ones used in classification. [20]. Probability that a given pixel will appear on the ground as it is classified (user accuracy) and the percentage of a given class that is correctly identified (producer accuracy) are separately calculated for supervised and unsupervised classification results. The classification accuracies for burned and damaged forest classes as well as the overall accuracy for both classifications are displayed in Table 6.1.
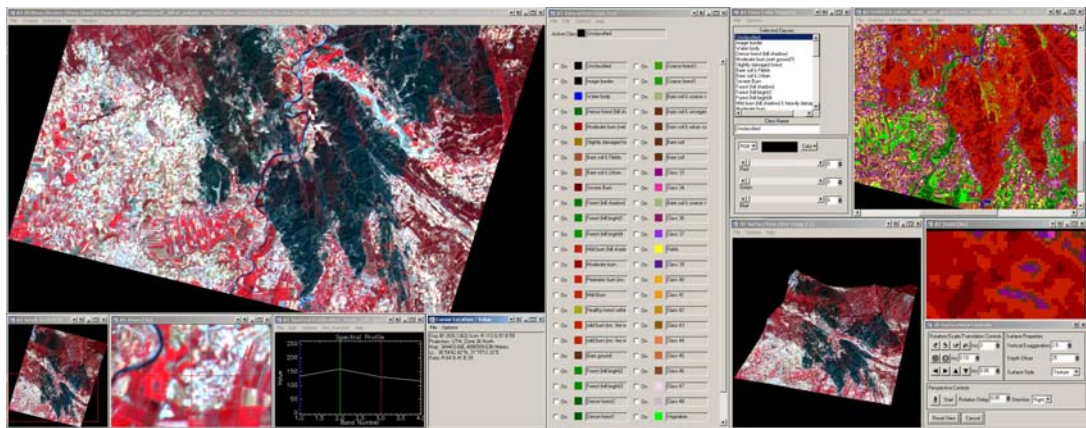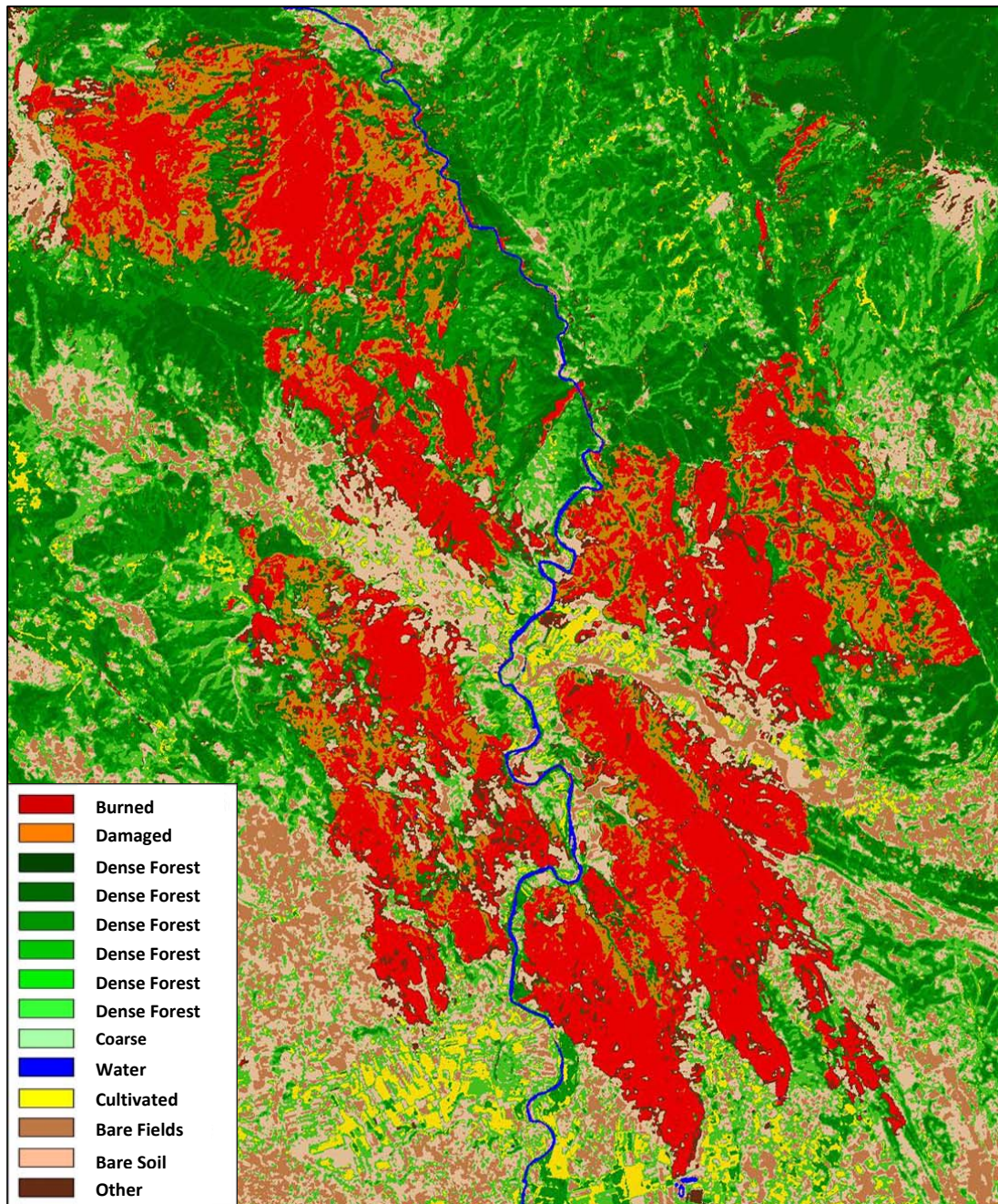
Table 6.1: Accuracy assessments for classification results

	Burned Forest Class		Damaged Forest Class		Overall Accuracy
	Producer Accuracy	User Accuracy	Producer Accuracy	User Accuracy	
Supervised Classification	% 98.68	% 92.35	% 80.07	% 90.77	% 81.28
Unsupervised Classification	% 98.93	% 97.90	% 96.15	% 98.06	% 96.24

When results were analyzed, it was observed that ISODATA unsupervised classification provided higher classification accuracy then maximum likelihood supervised classification for both burned and damaged forest classes. This is mainly due to the maximum likelihood classifier mixing the damaged forest spectra with healthy forest. Since supervised classification operates according to training data, similarity in training classes of healthy vegetation and damaged vegetation; both having higher reflectance in near infrared band than red band, had caused the classifier to confuse these classes resulting with a significance accuracy difference. Hence, supervised classification results were not used for later stages of the analysis.

6.6 Geometric Correction

For accurate acreage calculations and integration with other data, the geometrically distorted raw image had to be related to a reference system and coordinated. In this study, the data set was geometrically corrected using 1:25,000 scaled digital topographic maps in ED50 datum, having UTM projection. 15 ground control points were homogeneously and identically chosen from both images (Figure 6.11). First degree affine transformation was then applied with ± 0.75 pixels RMS error. Then

the same transformation parameters were applied to the classified images. Resampling method was chosen as Nearest Neighbor so original values would not be altered but replaced with newly corresponding cells after the transformation (Figure 6.12).

Figure 6.11 : Ground control points selection

a) Post fire image   b) Unsupervised classification

Figure 6.12 : Rectification results

6.7 GIS Analysis

As an objective of this study, it was desired to query the area of burned and/or damaged forest through post fire image classification results by integrating with the local forest management data, which contains a detailed database regarding variation in biomass and condition. In order to perform such a query, both data should be related under a similar geographic attribute. Thus the classification result and the local management data are evaluated under ArcGIS software.

In order to form an attribute relation, the records should consist of similar data types; however the classification results was in raster format and management data was made up of polygons; a vector format. In order to overcome this problem; initially, the current forest management plans made up of stance polygons in vector format were converted into raster format of pixels. Then each pixel in every stance polygon was related with the corresponding pixel of the classified image of the same coordinate, sharing their attributes, i.e. management information including the detailed species, age, growth condition, health, etc. (Figure 6.13 and Figure 6.14). Finally, a quarry consists of burned and damaged forest classes and tree types for each local chieftaincy was performed, extracting the information about the specific amount and distribution of damage done by the fire in terms of forest management (Table 6.2).
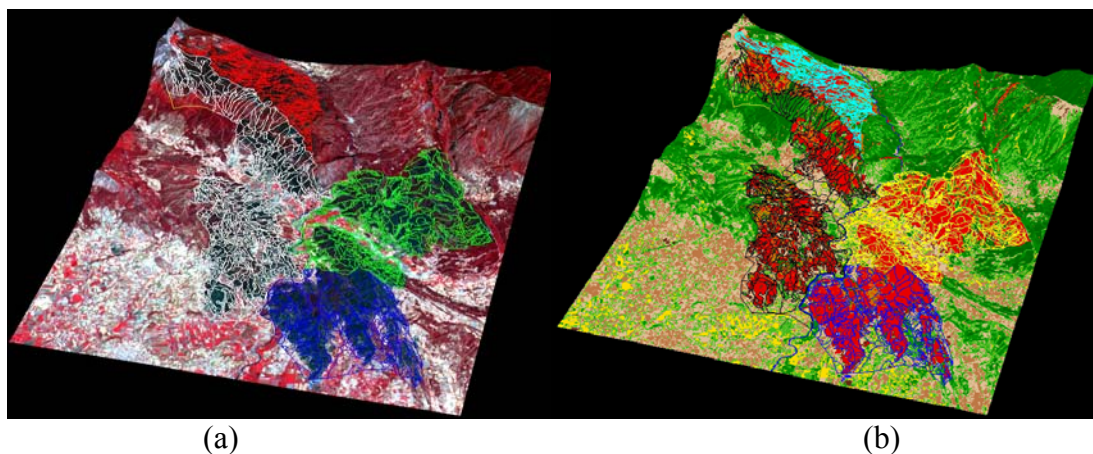

(a)   (b)

Figure 6.13 : Integration of local management and SRTM DEM layers
a) Rectified post fire image b) classification image

Figure 6.14 : Fire damage analysis with local management data within ArcGIS

Table 6.2: Query for the individual areas of burned and damaged stances

Stance Code	Burned forest area (ha)	Damaged forest area (ha)	Detailed Stance Report
BÇz	443,72	210,24	Rough Red Pine groand stance
BÇzM-T	14,36	21,12	Red Pine and Maple rocky mixed groand stance
BÇz-T	305,28	104,44	Rough and rocky Red Pine groand stance
Çz0Y	4,64	0,52	Spaced burned pure Red Pine stance
Çz0	2,36	3,36	Spaced pure Red Pine stance
Çza	832,76	98,4	Youth aged pure Red Pine stance
Çza0	342,00	27,32	Spaced youth aged pure Red Pine stance
Çza2	18,44	35,08	Mid closed youth aged pure Red Pine stance
Çza3	113,60	12,44	Fully closed youth aged pure Red Pine stance
Çzab2	2,88	0	Mid closed youth and log aged pure Red Pine stance
Çzab3	931,96	142,2	Fully closed youth and log aged pure Red Pine stance
Çzb3	280,76	109,28	Fully closed log aged pure Red Pine stance
Çzbc1	15,04	8	Loosely closed log and thin tree aged pure Red Pine stance
Çzbc2	60,08	19,52	Mid closed log and thin tree aged pure Red Pine stance
Çzbc3	666,08	253,6	Fully closed log and thin tree aged pure Red Pine stance
Çzc1	132,40	42,84	Loosely closed thin tree aged pure Red Pine stance
Çzc1-T	23,80	2,64	Loosely closed thin tree aged rocky Red Pine stance
Çzc2	158,40	99,84	Mid closed thin tree aged pure Red Pine stance
Çzc2-T	14,80	7,24	Mid closed thin tree aged rocky Red Pine stance
Çzc2Y	0,80	1,04	Mid closed thin tree aged burned Red Pine stance
Çzc3	417,72	171,48	Fully closed thin tree aged pure Red Pine stance
Çzcd1	74,76	71,04	Loosely closed thin, Mid and thick tree aged pure Red Pine stance
Çzcd2	497,08	250,28	Mid closed thin, Mid and thick tree aged pure Red Pine stance
Çzcd2-T	0,64	0	Mid closed thin, Mid and thick tree aged rocky Red Pine stance
Çzcd3	1725,64	889,8	Fully closed thin, Mid and thick tree aged pure Red Pine stance
Çzd	38,96	0	Mid and thick tree aged pure Red Pine stance
Çzd1	101,44	25,6	Loosely closed Mid and thick tree aged pure Red Pine stance
Çzd2	219,56	153,44	Mid closed Mid and thick tree aged pure Red Pine stance
Çzd3	192,00	237,68	Fully closed Mid and thick tree aged pure Red Pine stance
BÇn	4,16	2,16	Rough Eastern Plane stance
BDy	80,60	0,04	Rough other leaf tree stance
BKBt-T	251,48	185	Rough mixed swamp and Rocky meşcere
İs	1,96	0,52	Urban - cemetery
Ku-T	1,12	0,44	Sandy and Rocky mixed terrain
OT	11,08	4,88	Bare forest soil
OT-T	0,76	0,56	Rocky and Bare forest soil
T	21,60	16,64	Rocky terrain
Z	371,76	37,92	Agriculture terrain
Total	**8376,48 ha**	**3246,60 ha**	**Total affected area: 11623.08 ha**

Additionally to this study, a second post fire SPOT 4 image of the same region acquired on November 9th 2008 was also processed and evaluated (Figure 7.3) in order to observe the clean up and rehabilitation process however, it was seen that almost all of the so seemed damaged but alive forest area were indeed dead and cleaned up.

<div align="center">(a)   (b)   (c)</div>
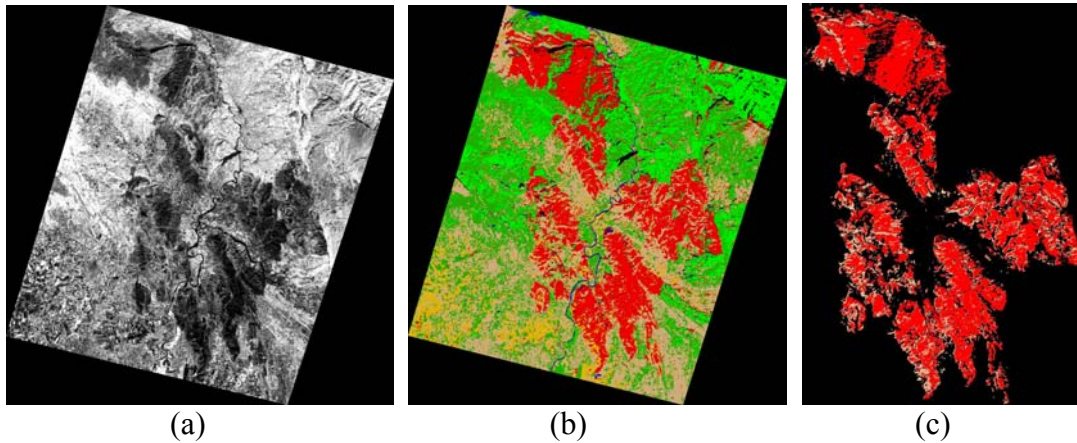
Figure 6.15 : November 9th, post fire image processing and classification
a) NDVI Image b) classification image c) Management areas

Besides, it was also realized that in many regions ground and surface fires were effective without a crown fire. Thus the canopies seemed healthy in the image right after the fire but as the trunk was burned, the trees were already dead in 3 months so according to the classification results, the burned forest area was calculated as increased amount of 10715.50 ha.

7. CONCLUSION

Hazard monitoring and evaluation have been a significant issue of remote sensing applications. Forest fires being the most frequent hazard, are vital ecological crises both internationally and in Turkey, thus should be seriously evaluated in terms of damage assessment and regeneration monitoring. Turkey having 21.2 million ha of forestland, of which 12 million ha being susceptible to fires mostly at Mediterranean regions; has suffered the loss of 1582590 hectares of forest land, due to 82556 forest fires from 1937 to 2007, consuming the forest land annually resulting in high suppression costs and loss in economy, ecology and even human life.

In knowledge of such experiences, Turkey's forests have to be strictly monitored against fires. Quick response should be given in case of a fire, for accurately planning the containment and extinguishing procedures. Periodic monitoring of previously burned forest areas have to be performed; to effectively intervene in case of arson scenarios for personal gain in urbanization, and to make rehabilitation as fast as possible. To accomplish these necessities by means of conventional methods, lot of time and manual labor are required thus it seems impossible to satisfactorily manage, however advancement in technology make it possible to detect, contain, analyze and monitor every stage of a forest fire faster, more accurate and recursively for either large or small areas.

Thus advanced technologies such as remote sensing technology involving mid / high resolution satellites with visible and infrared sensors, as well as Geographic Information Systems (GIS) providing an infrastructure to combine, analyze and query various data at the same time should be utilized in order to effectively evaluate the outcomes of a forest fire. Especially for stages of containment, damage analysis and monitoring, images acquired from remote sensing satellites help to provide synoptic data with rich spatial and spectral information. By means of this information as layers in combination to the available data within a GIS, a database for further inquiry of the damage can be provided cost effectively and hastily.

The major objective of this study was to analyze and authenticate the burned area due to the wildfire on dates between July 31st & August 5th, 2008 at Manavgat and Serik districts of Antalya, Turkey; by means of SPOT 4 satellite images and feature extraction techniques of remote sensing. Initially, spectral characteristics of the post fire vegetation were analyzed by means of a SPOT 4 multispectral satellite image acquired on August 7th. Three major outcomes in the forest ecosystem due to fire were observed as "alive and healthy", "partially burned but alive" and "burned" areas. Next, in order to enhance the differentiability, normalized difference vegetation index transformation was applied to the image data set, enhancing the green vegetation spectra proportional to its biomass and health. The NDVI data is then added to the original data set as a unique spectral band, and altogether processed and classified to extract the burned and partially damaged forest areas. Post-classification accuracies were calculated using independent control points and evaluated within a confusion matrix deriving user's and producer's accuracy percentages.

The unsupervised classification image with higher accuracy was geometrically transformed according to the map coordinates of the fire zone then affected areas were calculated as 3651.20 ha partially damaged but alive forest and 8580.56 ha of burned forest with a total of 11623.08 ha. The classification image was then associated with the local forest management data within ArcGIS to query the burned and damaged forest area with respect to tree types and stance attributes. It was observed that the most damage was done in fully closed, red pine stances.

This experience has made a point clear that, fire type and image acquisition date have a very important role in correct assessment of fire damage by classification of remote sensing images. Ground and surface fires affect the root and the trunk of the trees while leaving the canopy unharmed for the time being. However within a week the canopy dies as well. Thus in such cases, analysis of the remote sensing images; having data in visible and near infrared spectrums which only contain the information about to the top most surface of its target, acquired within a few days right after the fire can be misleading in exact calculation of the damage. If the purpose is to quickly portray the boundary of the fire zone and calculate an average amount of damaged area most recent images could be used; however in case of detailed analysis and accurate calculations of fire damage by means of remote

sensing, images with at least two weeks subsequent to the extinguished fire should be taken into consideration.

When classification results were compared with borderlines of the local management data drawn by General Directorate of Forestry, a 204.08 ha of burned and 404.60 ha of damaged area difference were observed. This difference is assumed to rely on several factors both possible errors in classification process and in conventional methods of General Directorate of Forestry. The conventional method which General Directorate of Forestry uses is simply, flying over the fire zone with a helicopter and a map technician hand drawing the burned area concurrently. This method most likely lacks accuracy and may result in miscalculation of the actual area, which is similar in this case. On the other hand, as SPOT 4 image has 20 meter spatial resolution; each pixel corresponds to 400 m² of area where mixed pixel phenomenon is likely to occur, especially in partially damaged forest area. Relief and shadow factor also complicates the classification, where a spectral reflection of the shadow could be confused with damaged forest spectra. Thus in order to improve the classification results, further classification techniques such as hybrid classification in which the results of the unsupervised classification are used as input values for the supervised classification process, could be utilized to increase the classification accuracy.

As accomplished with this study, advanced technologies such as remote sensing and Geographic Information Systems provide significant opportunities in detection, assessment and analysis of natural hazards. Either caused naturally or intentionally, wildfires tend to result in catastrophic damage to both environment and human beings. Global policies tend to utilize remote sensing increasingly, as the ultimate source of fast, accurate, synoptic data about any geographic event. When effectively analyzed and combined with ancillary data through a GIS, cases such early detection, containment, extinguishing, damage assessment and regeneration monitoring can easily and effectively be managed. Furthermore, scenarios can be developed and used as a training media to stay ready in case of similar emergencies.

Turkey being a country with 27 percent of its terrain as forestland and 49 percent of it classified as non productive, needs to take more care of its resources; when especially a significant distribution is concentrated in Mediterranean regions, being highly susceptible to fire. While racing against developing countries, Turkey needs to

standardize employing GIS and remote sensing technology for hazard management especially in fire monitoring and assessment. In competence in collection and updating of primary and ancillary data should be recognized and improved. Additional meteorological stations should be built particularly in fire susceptible regions. Data about forest condition including humidity, fuel load, age and closeness should be regularly collected and updated within a national forest information system. Furthermore, fire risk models should be derived using up to date data, not only to detect or to analyze the already done damage but also to model and simulate potential dangers and act accordingly, or rehabilitate and re-grow enriching the country's assets and improving welfare. To sum up, particular efforts to utilize GIS and remote sensing are personally being made however, without effective research and development, proper coordination between academic and administrative level and increase in government investments, thus change in the policy; a consistent advancement could not come true.

REFERENCES

[1] **FAO**, Food and Agriculture Organization of the Unites States, 2011, "Forestry" <http://www.fao.org/forestry/en/>, accessed 18.04.2011

[2] **CCRS,** Fundamentals of Remote Sensing <http://www.ccrs.nrcan.gc.ca/resourc e/tutor/fundam/index_e.php>, accessed 15.04.2011

[3] **NASA,** Electromagnetic Spectrum <http://science.hq.nasa.gov/kids/imagers/ems /gamma.html>, accessed 15.04.2011

[4] **Hyperphysics,** Infrared, <www.hyperphysics.phy-astr.gsu.edu/hbase/ems3.html> accessed 5.04.2011

[5] **Schneider, David J.,** Michigan Technological University Department of Geological Engineering and Sciences <www.geo.mtu.edu/rs/back /spectrum>, accessed 15.04.2011

[6] **Agouris, P.,** 2005., University of Maine, Energy Interactions <www.spatial. maine.edu/~peggy/Teaching/Ch1_B.ppt>, accessed 15.04.2011

[7] **Uwaterloo,** 2000., Environmental Remote Sensing. <www.fes.uwaterloo.ca /crs/geog165/scopers.htm>, accessed 15.04.2011

[8] **ENVI**, <http://geog.hkbu.edu.hk/virtuallabs/RS/env_backgr_refl.htm>, accessed 16.04.2011

[9] **Liew S. C.,** 2001 Centre for Remote Sensing and Processing, Principles of Remote Sensing, www.crisp.nus.edu.sg/~research/tutorial/rsmain.htm accessed 16.04.2011

[10] **Calgary,** <www.ucalgary.ca/UofC/faculties/SS/GEOG/Virtual/remoteintr.html> accessed 16.04.2011

[11] **Geoscience,** Earth Observation and Satellite Imagery, <www.ga.gov.au/acres/ prod_ser/sensor.jsp>, accessed 17.04.2011

[12] **CNES**, SPOT 5, <http://www.spot5.cnes.fr/gb/programme/programme.htm>, accessed 16.04.2011

[13] **CRISP**, NOAA Polar Orbiting Operational Environmental Satellite <http://crisp .nus.edu.sg/~research/tutorial/noaa.htm>, accessed 16.04.2011

[14] **Grahm S.,** 2011, Aqua Project Center <http://aqua.nasa.gov/about/instrument _modis.php>, accessed 16.04.2011

[15] **Maccherone B.,** Modis Design concept <http://modis.gsfc.nasa.gov/about/ design.php>, accessed 16.04.2011

[16] **Maccherone B.,** National Aeronautics and Space Administration: About Modis <http://modis.gsfc.nasa.gov/about/>, accessed 16.04.2011

[17] **NESPAL,** National Environmentally Sound Production Agriculture Laboratory <http://web.archive.org/web/20060901084006/nespal.cpes.peachnet.edu/pa/home/main.asp?TargetDir=25&content=4&media=>, accessed 18.04.2011

[18] **NRRI**, 2000, Normalized Difference Vegetation Index <http://oden.nrri.umn.edu/lsgis/ndvi.htm>, accessed 18.04.2011

[19] **RNCAN,** Remote Sensing Tutorial <http://cct.rncan.gc.ca/resource/tutor/fundam/chapter4/07_e.php>, accessed 19.04.2011

[20] **Storm,** Accuracy Assessment Exercise <http://web.archive.org/web/20040302114453/http://www.storm.uni.edu/rs/2001/ars/accuracy/>, accessed 18.04.2011

[22] **Flannigan,** Forest Fires and Climate Change in the 21st century. *Mitigation and Adaptation Strategies for Global Change.* 2005 <https://www.firelab.utoronto.ca/pubs/2005_flannigan_wotton_etal.pdf>, accessed18.04.2011

[23] **Krock,** Lexi., June 2002 NOVA online Public Broadcasting System (PBS). The World on Fire; <http://www.pbs.org/wgbh/nova/fire/world.html>, accessed 18.04.2011

[24] **Forest Fires**, An Overview <http://www.borealforest.org/world/innova/forest_fire.htm>, accessed18.04.2011

[25] **Dosomething,** 11 Facts About Wildfire, <http://www.dosomething.org/tipsandtools/11-facts-about-wildfire>, accessed 18.04.201

[26] **Wildfires** <http://environment.nationalgeographic.com/environment/naturaldisasters/wildfires/>, accessed 18.04.2011

[27] **NWCG**, April 2006, National Wildfire Coordinating Group, Fire line Handbook, Appendix B: Fire Behavior <http://.nwcg.gov/pms/pubs/4102/appendixB.pdf>, accessed 18.04.2011

[28] **NIFC**, *National Wildfire Coordinating Group Communicator's Guide For Wildland Fire Management*, 3.<http://www.nifc.gov/preved/comm_guide/wildfire/FILES/PDF%20%20FILES/Linked%20PDFs/2%20Wildland%20fire%20overview.PDF>, accessed 20.04.2011

[29] **US Forest Service**. Influence of Forest Structure on Wildfire Behavior and the Severity of Its Effects; November 2003 <http://www.fs.fed.us/projects/hfi/2003/november/documents/forest-structure-wildfire.pdf>, accessed 20.04.2011

[30] **NWCG**, *Glossary of Wildland Fire Terminology*, p.74. www.nwcg.gov/pms/pubs/glossary/pms205.pdf accessed 23.04.2011

[31] **de Souza Costa**, **F.**; Sandberg, D., Mathematical model of a smoldering log .*Combustion and Flame.* 2004 <http://www.fs.fed.us/pnw/pubs/journals/pnw_2004_costa001.pdf>, accessed24.04.2011]

[32] **Billing, P**. 1983, Victoria Department of Sustainability and Environment. Otways Fire No. 22 - 1982/83 Aspects of fire behavior. Research Report No.20; <http://www.dse.vic.gov.au/CA256F310024B628/0/97 892B7CD0C75AB3CA2572230047B454/$File/Research+Report+20. pdf >, accessed 24.04.2011

[33] **Forestencyclopedia,** Types of Natural Fires: Surface Fires, Ground Fires, and Crown Fires <http://www.forestencyclopedia.net/p/p1464>, accessed 24.04.2011

[34] **CBC**, Radio communication keeps rangers in touch <http://archives.cbc.ca/ver sion_print.asp?page=1&IDLan=1&IDClip=4917&IDDossier=849&I DCat=346&IDCatPa=261>, accessed 27.04.2011

[35] **Disastercenter,** An Integration of Remote Sensing, GIS, and Information Distribution for Wildfire Detection and Management, *Photogrammetric Engineering and Remote Sensing*. October 1998 <http://www.westerndisastercenter.org/DOCUMENTS/PERS_PAPER .pdf>, accessed 27.04.2011

[36] **Fok**, Chien-Liang; Roman, Gruia-Catalin; and Lu, Chenyang. Washington University in St. Louis. Mobile Agent Middleware for Sensor Networks: An Application Case Study [PDF]; 2004-11-29 <http://web.archive.org/web/20070103233730/http:/cse.seas.wustl.edu /techreportfiles/getreport.asp?399>, accessed27.04.2011

[37] **Thomson**, Elizabeth A. Massachusetts Institute of Technology (MIT) News. Preventing forest fires with tree power; 2008, <http://web.mit. edu/newsoffice/2008/trees-0923.html>, accessed 27.04.2011

[38] **San-Miguel-Ayanz**, Jesus; Ravail, Nicolas; Kelha, Vaino; Ollero, Anibal. Active Fire Detection for Fire Emergency Management: Potential and Limitations for the Operational Use of Remote Sensing *Natural Hazards*. 2005 <http://grvc.us.es/publica/revistas/do cumentos/R-050.05ActiveFire.pdf>, accessed 27.04.2011

[39] **Dempsey, C.,** GIS Lounge: What is GIS? <http://gislounge.com/what-is-gis/>, accessed 27.04.2011

[40] **ESA,**. 2006,Earth from Space: California's 'Esperanza' fire; <http://www.esa .int/esaEO/SEMEKMZBYTE_index_0.html>, accessed 27.04.2011

[41] **CWFIS,** Canadian Forest Fire Behavior Prediction System <www.cwfis.cfs.nrc an.gc.ca/en_CA/background/summary/fbp> accessed 27.04.2011

[42] **Britta** A., Reto S., Forest Fire Modelling with GIS in the Swiss National Park <www.ncgia.ucsb.edu/conf/SANTA_FE_CD-ROM/sf_papers/allgowe r_britta/allgower.html>, accessed 27.04.2011

[43] **Min L.,** John J. Q., Xianjun H. Estimating aboveground biomass for different forest types based on Landsat TM measurements <http://ieee xplore.ieee.org/xpl/mostRecentIssue.jsp?punumber=5286203>, accessed 27.04.2011

[44] **Huai K. K.,** Use of Landsat TM to Detect Change in Tropical Forest Types After Fire <http://ieeexplore.ieee.org/xpl/freeabs_all.jsp?arnumber=1 469834>, accessed 27.04.2011

[45] **Sun G.;** Rocchio L.; Masek J.; Williams D.; and Ranson K. J.; Characterization of Forest Recovery From Fire Using Landsatand SAR Data http://ieeexplore.ieee.org/xpl/freeabs_all.jsp?arnumber=1025780 accessed 27.04.2011

[46] **NOAA,** Satellite and Information Service. Hazard Mapping System Fire and Smoke Product <http://www.osdpd.noaa.gov/ml/land/hms.html>, accessed 27.04.2011

[47] **Buck A**.; Kok R.; Schneider T.; Ammer U.; Improvement of a forest GIS by integration of remote sensing data for the observation and inventory of "protective forests" in the Bavarian Alps <www.earth.esa.int/ pub/ESA_DOC/gothenburg/327schne.pdf>, accessed 27.04.2011

[48] **Liu W.;** Wang S.; Zhou Y.; Wang L.; Zhang S., Analysis of Forest Potential Fire Environment Based on GIS and RS <www.ieeexplore.ieee.org/ie l5/5559273/5567473/05567966.pdf?arnumber.3D5567966&authDecis ion=-203>, accessed 27.04.2011

[49] **UNISDR,** United Nations International Strategy for Disaster Reduction, The Global Wildland Fire Network: Regional South East European / Caucasus Wildland Fire Network: COUNTRY REPORT TURKEY <www.rfmc.mk/pdf/Turkey/Country-Fire-Report-Turkey.pdf>, accessed 27.04.2011

[50] **Ün, C.**, Coğrafi Bilgi Sistemlerinin Orman Yangınlarında Kullanımı, 1. Orman Yangınları ile Mücadele Sempozyumu, 7-10 Ocak 2009

[51] **TMMOB**, *Doğal Kaynaklar Orman, Çevre ve Maden.* <http://www.tmmob.org .tr/genel/bizden_detay.php?kod=3215&tipi=16>, accessed 28.04.2011

[52] **Vikipedi,** 2008, *Serik, Antalya.* Source: <http://tr.wikipedia.org/wiki/Serik>, accessed 28.04.2011

[53] **Antalya**, 2008, *Antalya: Manavgat, Genel Bilgi.* <http://www.antalyakult urturizm.gov.tr/belge/1-71522/eski2yeni.html>, accessed 28.04.2011

[54] **SPOT Image,** Preprocessing Levels and Location Accuracy <http://www.sp otimage.com/web/en/234-preprocessing-levels-and-location-accuracy. php>, accessed 28.04.2011

[55] **Weier, J.;** Herring, D., 2008, *Measuring Vegetation.* Source: <http://eartho bservatory.nasa.gov/Features/MeasuringVegetation/printall.php>, accessed 28.04.2011

[56] **CCRS,** Glossary of remote sensing terms <http://www.ccrs.nrcan.gc.ca/glo ssary/index_e.php?id=341>, accessed 29.04.2011

[57] **Yale,** Unsupervised Classification <http://www.yale.edu/ceo/Projects/swap/lan dcover/Unsupervised_classification.htm>, accessed 29.04.2011

CURRICULUM VITAE

KEREM ESEMEN

Address:	TRT Basın Sitesi, M Blok B Kapısı
	Daire: 11 Yenilevent, İstanbul - Turkey
Phone (mobile):	+90 535 770 9409
Phone (home):	+90 212 268 6848
E-mail:	keremesemen@gmail.com

Personal Information
Birth Date:	12/09/1984 İstanbul, Turkey
Non-smoker	

Educational Profile
University:	İstanbul Technical University (2008 – 2011)
Institute:	Informatics Institute
Department:	Satellite Communications & Remote Sensing M.Sc.
University:	İstanbul Technical University (2004 – 2008)
Faculty:	Civil Engineering Faculty
Department:	Geomatics Engineering
University:	İstanbul Technical University (2002 – 2004)
Faculty:	Aeronautics and Astronautics Engineering Faculty
Department:	Aerospace Engineering
Junior & Senior High:	Üsküdar American Academy (1995 – 2002)
Primary:	Özel Yüzyıl Işıl Primary School (1990 – 1995)

Language Skills
Turkish	Native Fluency
English	Native Fluency
German	Basic Knowledge

Computer Skills
Programming	C / C++, FORTRAN
Tools	ENVI, ArcGIS, PCI Geomatica
	NetCAD, AutoCAD
	Microsoft Office tools, Adobe: Photoshop, Acrobat Professional

Career Interests

Remote Sensing, Image Processing, Geographic Information Systems

Work Experience

İstanbul Technical University:
Center For Satellite Communications and Remote Sensing (ITU–CSCRS)
Worked as intern and researcher at İTÜ Center for Satellite Communications & Remote Sensing, on post-fire analysis and damage evaluation.
February 2008 – February 2009

İstanbul Technical University:
Geomatics Engineering Dept. of Remote Sensing
Worked as student assistant within TÜBİTAK project #106K350 on the study of Roman and Byzantine water transport system through Thrace to former Constantinople (İstanbul) by means of Remote Sensing and surface archeology techniques.
January 2007 – January 2008

TÜBİTAK Marmara Research Center:
Earth and Marine Sciences Institute
Worked as intern at TÜBİTAK Marmara Research Center on application of remote sensing in earth sciences.
26 June – 14 July, 2006

Publications

EARSeL 2009
Sunar F., **Esemen K**., Özkan C. (2009)
Post-Fire Evaluation Using SPOT 4 Satellite Images,
European Association of Remote Sensing Laboratories Symposium.
15 – 18 June 2009, Crete - Greece

1st Symposium on Campaign Against Forest Fires
Sunar F., **Esemen K**. (2009)
Uydu Görüntüleri ile Orman Yangını Analizi,
1st Symposium on Campaign Against Forest Fires.
07 – 10 January 2009, Antalya - Turkey

2nd Remote Sensing and GIS Symposium, 2008
Esemen K., Sunar F. (2008)
Spot 2 Uydu Görüntüleri ile Orman Yangını Analizi: Bodrum Örneği,
2nd Remote Sensing and GIS Symposium.
13 – 15 October 2008, Kayseri - Turkey

Esemen K., Güçin M., Sunar F., Yavuz V. (2008)
Uydu Görüntüleri ile Karlı Alan Değişim Analizi: Kaçkar Örneği,
2nd Remote Sensing and GIS Symposium.
13 – 15 October 2008, Kayseri - Turkey

Social Activities and Hobbies

Conductor at Istanbul Soundtrack Orchestra (İstanbul Film Müzikleri Orkestrası)
Principal flutist at Pera Youth Orchestra (Pera Gençlik Orkestrası)
Guitarist at Mutlak Sessizlik music band
Radio controlled model aircraft building and piloting